

Observing Jovian Decametric Radio Emissions with a Software Defined Radio Telescope

David Kirwan, Dr. Alan Davy*, and John Ronan*

Waterford Institute of Technology,
Dept of Computing and Mathematics,
Cork Rd, Waterford City, Ireland
dkirwan@tssg.org
<http://www.wit.ie>

Abstract. The planet Jupiter emits in the radio spectrum strongly in the $10 - 100m$ wavelength range. A low cost radio telescope based on NASA's Radio Jove design was built to capture frequencies within this range. A HackRF radio transceiver was used to allow data collection, while a software defined radio solution was implemented in GNURadio to perform data processing with the hope of capturing these Jovian emissions. Several utilities were developed to aid in the analysis of captured data. As the cost of software defined radio receivers fall and the availability of free open source software becomes more prevalent, capabilities once available only to government institutions or large universities are now within reach of the determined amateur enthusiast.

Keywords: radio astronomy, software defined radio, digital signal processing, gnuradio, hackrf

* Supervisors

Acknowledgements

This dissertation would not have been possible without the support of the following people.

To my supervisors Alan and John for their patience, guidance and sharing of knowledge during this process. Thank you, it has been a real pleasure working together.

To my lecturers at the Waterford Institute of Technology, you have all been so open and free with your sharing of knowledge, it has been an absolute pleasure learning from you.

To my partner Michael, I'm keenly aware standing in the freezing cold at 02:00 helping me put up radio antennas might not have been the most exciting thing you've partaken in all year, but I couldn't have done it without your help. Thanks for your constant encouragement and for putting up with me during this.

To my sister Jean, you inspired me to work as hard as I have these last 6 years. I wanted to make you as proud of me as I am of you. If you beat me to Ph.D, I'll buy you a bag of chips in Roccos.

To my father, I can only imagine the conversations we might have had, I suspect you would have loved playing with this equipment as much as I have.

To my mother, thank you for your friendship. You have always been a positive influence in my life. Some day you must sit down and explain how you can walk past, and in the time it takes to cross a room and without any prior involvement, solve a problem I have been struggling with for days.

To my four dogs Noah, Oscar, Rosie and Dora, you are the best mutts a man could ask for.

Table of Contents

Observing Jovian Decametric Radio Emissions with a Software Defined Radio Telescope	1
<i>D. Kirwan</i>	
Glossary	4
List of Figures	7
List of Tables	8
Introduction	9
Research Hypothesis	15
Methodology	17
Research Questions	19
Literature Review.....	20
Testbed Build and Verification	25
Special Resources Required.....	25
Antenna Build.....	26
Listening Site Suitability	29
Verification of the Radio Receiver	31
Capturing DAM Emissions	36
Research Question 1	38
Determine SDRT Power Requirements	38
Determine SDRT Computational Power Requirements	44
Determine SDRT Network Connectivity Requirements	45
Research Question 2	47
Flag Amateur Radio Enthusiast Transmissions.....	47
Flag Natural Emission Sources.....	50
Research Question 3	52
Capturing DAM Emissions with the RTL2832 DAB SDR	52
Implementing a HackRF Compatible Flow-Graph in GNURadio	56

Conclusions	60
Future Work	61
Filtering Human Signal Interference	61
Filtering Natural Interference	61
Creating Spectrograms with HackRF	62
Calibrating the SDRT for Accurate Power Measurements	62
Automated Detection of DAM Emissions	63
Final Summary	63
Appendices	64
Bibliography	70

Glossary

DAM decameter radio emissions in the 10-100 m wavelengths. 9, 11–20, 25, 26, 34, 36, 37, 52–54, 58, 60, 61, 63

DXCluster DXCluster - Number of DXServers connected together into a cluster, where amateur radio enthusiasts can share spotted instances of radio contact between each other. 48

HF High Frequency usually refers to radio frequencies in the 3 - 30 MHz. 11, 12

IFT Io Flux Tube is a cylindrical area of space containing magnetic field lines. 10, 20

IoT Internet of Things a buzzword for everything connecting to everything. 18, 19, 38, 60

IPT Io Plasma Torus is created by Jovian atmospheric electrons ionizing neutral atmospheric gas such as sulphur in orbit around Io. 9

IQ Imaginary Quadrature signal - Complex signal data and quadrature phase values in a digital signal sample. 19, 33, 52

LOFAR Low Frequency Array - radio interferometer constructed in the north of the Netherlands and across europe <https://www.astron.nl/lofar-telescope/lofar-telescope>. 29

preamp pre-amplifier - is an electronic amplifier that prepares a small electrical signal for further amplification or processing. 29, 34

RF Radio Frequency is a rate of oscillation which corresponds to the frequency of a radio wave. 29, 34

MW MW - Medium Wave frequencies usually in the wavelengths 300 kHz - 3 MHz. 6, 31–33

RSGB RSGB - The Radio Society of Great Britain <http://rsgb.org/>. 31

SDR Software Defined Radio is the creation of radio functions within software rather than hardware. 15, 17–19, 22, 25, 29, 33, 52, 61, 62

SWR Standing Wave Ratio is the ratio of the maximum peak voltage anywhere on a line to the minimum value anywhere along a line. 26, 27

List of Figures

1	Decametric Radio Emissions [Ashcraft, 2013]	9
2	Neutral Gasses in Orbit of Io [Belcher, 1987]	10
3	Magnetic Flux Tube linking Jupiter and its satellite Io [Belcher, 1987]	10
4	Alfvén Waves following Io through its orbit and the DAM Emission cones [Bose et al., 2008]	11
5	Irish Regulatory Transmission Ranges [Comreg, 2014]	12
6	Wavelength Equation	12
7	Wavelength Equation for Real World Half Wavelength Dipole Antenna	13
8	Wavelength Equation for Real World Half Wavelength Wire Antenna .	13
9	Ideal DAM Emissions types from Jupiter [Wilkinson and Kennewell, 1994]	14
10	Dual Dipole Antenna Beam at 20FT and 135deg phasing South [NASA, 2012b]	15
11	Dipole antenna characteristics and Jupiter's altitude.....	16
12	Dual Dipole Antenna Array [NASA, 2012b]	16
13	Sampling an Analogue Signal [Smith, 2003b]	21
14	Sampling Theorem aka Nyquist-Shannon sampling theorem [Smith, 2003b]	22
15	I/Q Samples Helix [Kuisma, 2014].....	22
16	I/Q Samples Polar Plot [Kuisma, 2014]	23
17	Measuring the SWR of the antenna with an SWR Analyser	26
18	Standing Wave Ratio Equations	27
19	Calculating P_r for the antenna	27
20	Site Survey.....	30
21	Comparing propagation of MW radio signals during day and during night/solar eclipse [Nichols, 2015a]	32
22	20th March 2015 solar eclipse.....	35
23	DAM Emissions	37
24	DAM Emissions	40
25	Calculating Amps using Watts and Voltage.....	41
26	Average Daily Sunshine in Waterford	42
27	Solar Plots	43
28	DXCluster Client Architecture	47
29	DXCluster data	49
30	Haversine Formula	51

31 Blitzortung data	51
32 24 - 28 MHz Spectrograms of rtl_power data plotted using heatmap.py	54
33 24MHz - 40MHz Spectrograms of rtl_power data plotted using heatmap.py	55
34 Converting in-phase and quadrature-phase to power values	56
35 Total Power Meter Implemented in GNURadio [Nelson, 2015]	56
36 Radio Skypipe Software Power Plot [Radio-Sky-Publishing, 2015]	57
37 Calibration of the SDR Radiometer	58
38 GNURadio flow-graphs to generate total power plots from saved data	59
39 Converting Power(V) to Temperature(K)	62
40 Calibration of Telescope Total Noise Power	63
41 A searchlight beam model of Jupiter's decametric radio emissions [Imai et al., 2008]	64
42 Io Flux Tube and the Plasma Torus [Lang, 2010]	64
43 21MHz Shortwave Loop Design	65
44 Distance between the Birr and Kilkenny site survey	66
45 Signal Modulation	66
46 Partial Solar Eclipse 20th March 2015 [timeanddate.com, 2015]	67
47 SDRT Dual Dipole Antenna Design based on NASA RadioJove	67

List of Tables

1	Most common types of DAM Emissions from Jupiter [Wilkinson and Kennewell, 1994]	14
2	Literature Review Synthesis Matrix	24
3	SDRT Build Cost	28
4	SDRT Build Cost [NASA, 2014]	29
5	Average Noise Measurements at Kilkenny Listening Site compared to Birr Listening Site [McCauley, 2013]	31
6	System Power Requirements	44
7	System CPU Power Requirements	45
8	Networking technologies transferring 2GB data	46
9	Sample DXSpider Data Packet	48
10	Sample Blitzortung Data Packet	50
11	RTL vs HackRF and SDRT Requirements	53

Introduction

It was discovered in 1954 by [Burke and Franklin \[1955\]](#) that the planet Jupiter emits radio transmissions in the decameter (DAM) range (10-100 m wavelengths), and the inner Jovian satellite Io appeared to have a strong control effect on these emissions [\[Belcher, 1987\]](#). Jupiter's radio emissions range between 4 MHz to 40 MHz while emitting most strongly at 8 MHz [\[Wilkinson and Kennewell, 1994\]](#). Due to interference from human short wave radio sources between 4-15 MHz coupled with the attenuation of these signals below 8 MHz or the refraction off Earth's ionosphere, the majority of emissions have been observed up in the 15-25 MHz range where this interference is less [\[Wilkinson and Kennewell, 1994\]](#). The emission signal strength quickly diminishes above this range for ground based listening sites [\[Wilkinson and Kennewell, 1994\]](#).

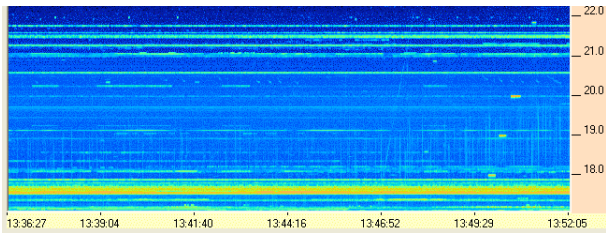


Fig. 1: Decametric Radio Emissions [\[Ashcraft, 2013\]](#)

Data collected by the two Voyager spacecraft in 1979 [\[Belcher, 1987\]](#) and the later Galileo mission in 1995 [\[Kivelson et al., 1996\]](#) added hugely to the understanding of the plasma interactions between Jupiter and Io and the source of the DAM emissions. It was discovered that the Io has a thin atmosphere made up of a number of neutral gasses namely sodium, potassium, sulphur, and oxygen as shown in Figure. 2 on page 10. It is generally thought these gasses have been emitted through volcanic activity on the surface of the moon [\[Belcher, 1987\]](#). The gasses in orbit of Io have a very short life time, due to collisions with magnetospheric electrons. This gives rise to a plasma torus (IPT) which co-rotates with Jupiter itself [\[Belcher, 1987\]](#). This can also be seen in Figure. 2 on page 10 which shows the IPT.

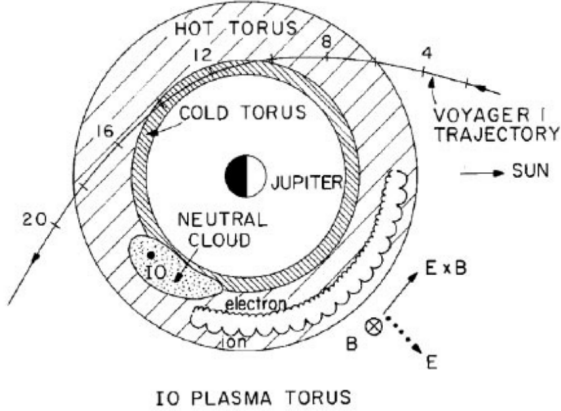


Fig. 2: Neutral Gasses in Orbit of Io [Belcher, 1987]

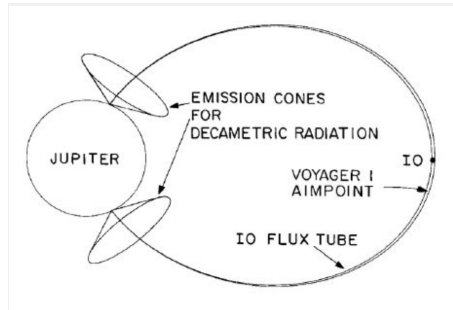


Fig. 3: Magnetic Flux Tube linking Jupiter and its satellite Io [Belcher, 1987]

The local co-rotation speed of the plasma torus is faster than the Keplerian orbit of the moon, and the plasma overtakes Io in its orbit at 57 km/s^{-1} [Belcher, 1987]. Figures. 3 and 42 on pages 10 and 64 detail diagrams of the Io Flux Tube (IFT) which is a cylinder shaped tube of space containing Jovian magnetic field lines [Belcher, 1987] which link Io to Jupiter's ionosphere at both poles. A large portion of the decametric emissions come from the area where this IFT meets the Jovian ionosphere [Belcher, 1987].

Io acts as a unipolar conductor as it orbits within this flux torus [Bose et al., 2008]. Alfvén waves are regularly produced which carry an electric charge along the magnetic field lines between Io and Jupiter [Bose et al., 2008] thereby acting as a standing wave [Bose et al., 2008]. These Alfvén waves reflect between

Jupiter's ionosphere at poles and Io up to 9 times [Bose et al., 2008] before dissipating as they follow Io through its orbit.

It appears the source of the DAM emissions are largely due to these reflections of the Alfvén waves off Jupiter's ionosphere in both the northern and southern regions [Bose et al., 2008]. See Figure. 4 on page 11 which shows the Alfvén wings reflecting from Jupiter's Ionosphere creating emission cones.

The DAM emissions radiate outwards in the shape of a cone as show in Figure. 3 on page 10 [Belcher, 1987]. When Io is at specific points in its orbit of Jupiter, these emission cones are pointing in the direction of Earth, at which point emissions can be picked up at ground based radio telescope listening stations.

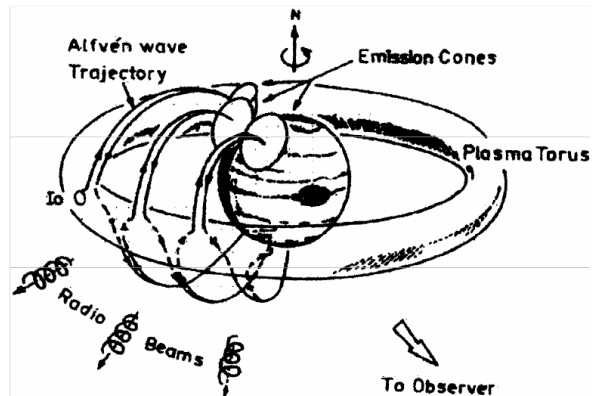


Fig. 4: Alfvén Waves following Io through its orbit and the DAM Emission cones [Bose et al., 2008]

A ground based listening station aiming to record DAM emissions from Jupiter is most likely to succeed between 15-25 MHz [Wilkinson and Kennewell, 1994]. According to ARRL [2000] there is no clear definition of the shortwave radio bands however it is most often considered to extend from 3 MHz to 30 MHz. ComReg is the Irish Commission for Communications Regulation within Ireland, and maintains a list of the short wave frequencies which are designated for transmission purposes in Ireland and can be seen in Figure. 5 on page 12 [Comreg, 2014].

As many commercial short wave radio stations transmit in the lower end of the high frequency (HF) 4 - 8 MHz range, it can be extremely busy and po-

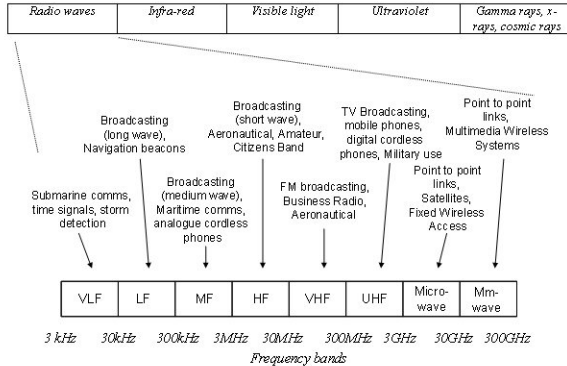


Fig. 5: Irish Regulatory Transmission Ranges [Comreg, 2014]

tentially difficult to monitor DAM emissions where they are strongest. Amateur Radio operators also operate frequently in mid-late HF ranges (160 m, 80 m, 60 m, 40 m, 30 m, 20 m, 17 m, 15 m, 12 m and 10 m bands) while the higher frequency DAM emissions taper off in strength very quickly. This limits the potential listening range significantly. Despite these obstacles, there are sections of the HF spectrum which are suitable to capture Jovian emissions. One frequency to monitor Jovian DAM emissions which is recommended by the Radio Jove project is 20.1 MHz [NASA, 2012b].

Sourcing a suitable antenna is one of the first requirements to satisfy in order to capture DAM emissions. Antennas are generally best suited to collect electromagnetic radiation at single specific frequencies, but may resonate and therefore operate over a range of frequencies depending on the design [NASA, 2012b]. The wavelength (λ) which corresponds with the frequency (f) 20.1 MHz can be obtained using the wavelength equation as shown in fig 6. The corresponding wavelength for the frequency 20.1 MHz works out to be 14.925 m using this equation.

$$\lambda = \frac{c}{f} \quad (1)$$

$$\lambda = \frac{3 \times 10^8 m/s}{20.1 \times 10^6 Hz} = 14.925373134328359 m \quad (2)$$

Fig. 6: Wavelength Equation

One simple antenna design for collecting DAM emissions is the dipole. A dipole antenna can be constructed simply and cheaply from two pieces of wire and three insulators [NASA, 2012b], while ensuring to cut the wires to a length matching half the desired wavelength being captured [NASA, 2012b]. However as the formula referenced in Figure. 6 on page 12 describes the use of an infinitely thin wire which is not possible in reality, capacitive end effects must be taken into account when working out the resonating wavelength for a dipole antenna [NASA, 2012b].

The formula for calculating the resonating frequency for a half wavelength dipole is described in Figure. 7 on page 13 and produces the value which should measure from tip to tip on the wires used to construct the dipole antenna [NASA, 2012b]. RSGB [2014] states in practice that the true resonance is not exactly multiples of the half-wavelength due to factors such as the coatings on the wire and loss due to radiation. A second formula is detailed in Figure. 8 on page 13 which takes these factors into account and produces an antenna length which is slightly larger than the formula proposed by [NASA, 2012b]. In Formula: 4 n stands for the number of half-wavelengths in the antenna.

$$\left(\frac{\lambda}{2}\right)m = \frac{142.65}{20.1MHz} = 7.097014925373134m \quad (3)$$

Fig. 7: Wavelength Equation for Real World Half Wavelength Dipole Antenna

$$\lambda m = 155 \left(\frac{n - 0.05}{f} \right) \quad (4)$$

$$\lambda m = 155 \left(\frac{1 - 0.05}{20.1MHz} \right) = 7.325870646766169m \quad (5)$$

Fig. 8: Wavelength Equation for Real World Half Wavelength Wire Antenna

The radio emissions come in several different forms each with slightly different characteristics. Table. 1 shows a list of the more widely known types which can be picked up using ground based listening equipment, and also has some in-

formation about their different characteristics [Wilkinson and Kennewell, 1994]. Any particular observation session might be made up of some or all of these different types of DAM emission and can last from a few minutes to several hours for larger noise storms [Wilkinson and Kennewell, 1994].

Type	Emission Length	Emission Description
S-Bursts	short generally 1-10 milliseconds	wideband bursts, several MHz wide
L-Bursts	long 0.5 - 5 seconds	wideband bursts, several MHz wide
N-Bursts	milliseconds upto seconds	narrowband bursts, several kHz wide

Table 1: Most common types of DAM Emissions from Jupiter [Wilkinson and Kennewell, 1994]

Figure. 9 on page 14 shows an ideal case of the S-Burst and L-Burst DAM emissions and what they might look like on a frequency spectrum graph. S-Burst emissions are short, generally $1-10 \times 10^{-3}$ s long while L-Bursts can often be between 0.5-5s in length.

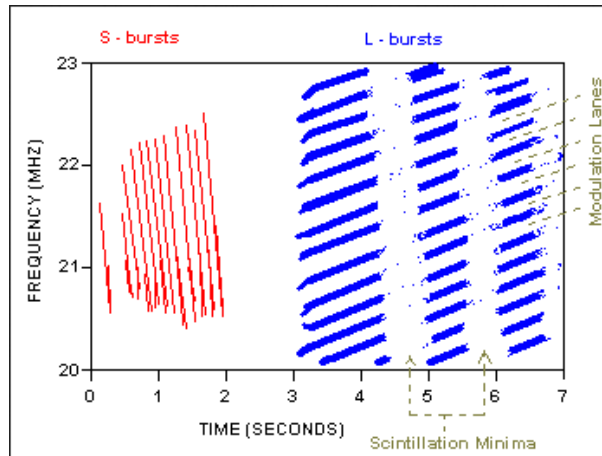


Fig. 9: Ideal DAM Emissions types from Jupiter [Wilkinson and Kennewell, 1994]

Research Hypothesis

The aim of this project is to design and construct a low cost, self sufficient software defined radio (SDR) telescope listening station, which can capture signals for transmission to a central data aggregation point for signal processing and analysis. This telescope should be suitable to study signals in the DAM (10-100 m) band at or near the 20.1 MHz frequency in order to pick up emissions produced by either Jupiter or the Sun.

There are a number of challenges which need to be overcome to achieve this, such as Jupiter only being visible for a number of months each year and then generally in the evening, night, or morning hours. Often at highly unsociable times. For this reason a radio telescope listening site should be as automated as possible.

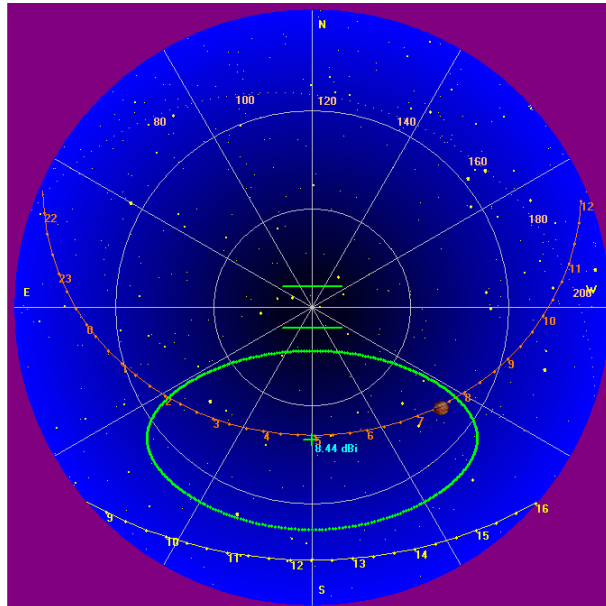


Fig. 10: Dual Dipole Antenna Beam at 20FT and 135deg phasing South [NASA, 2012b]

During daylight hours, the ionosphere becomes opaque to signals in the DAM band due to becoming ionised by solar radiation [NASA, 2012a]. The proposed system will have a short window in the order of 1-6 hours every second night and early morning. During which it may be possible to capture DAM emissions

from Jupiter. The Sun is a source of DAM emissions also, and the telescope can capture solar storm emissions without modification, providing the Sun passes through the antenna beam. The telescope may require manual reconfiguration in order to pick up solar storm emissions during the day.

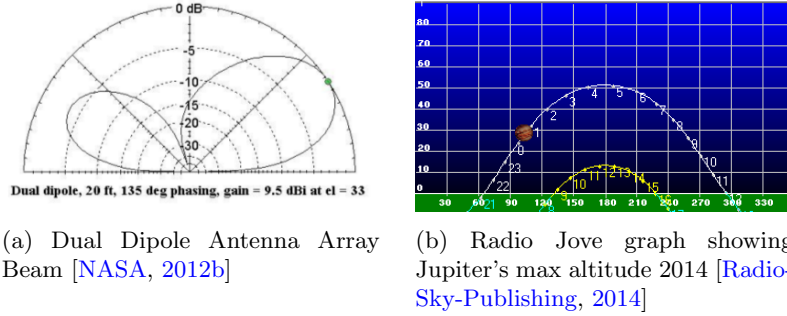


Fig. 11: Dipole antenna characteristics and Jupiter's altitude

Interference from human sources such as short wave radio stations or amateur radio operators are also likely to affect the collection of DAM emissions from Jupiter. The ability for automated flagging or removal of interference would be a desirable feature of the system. Lightning storms can also produce interference which will affect observations, it might be desirable for the system to handle natural interference sources also.

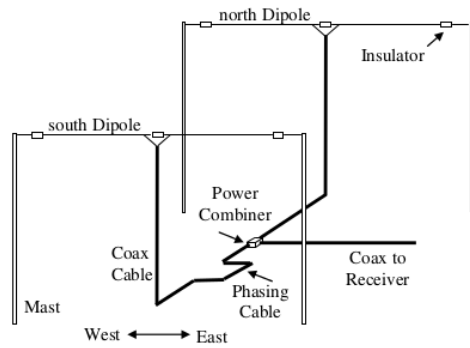


Fig. 12: Dual Dipole Antenna Array [NASA, 2012b]

Methodology

The section aims to provide a summary of the methodologies which will be followed on this project in order to answer the research questions put forward in the next section. It is broke up into the following subsections:

Antenna Build

Building the antenna is further broken down into the following steps:

- source materials to build a dual dipole antenna
- build the telescope antenna
- validate the antenna is capable of collecting signals at or near the 20.1 MHz frequency

Analysis of Listening Site Suitability

Finding a site suitable to deploy the antenna will require a site survey with the antenna connected to a spectrum analyser. The spectrum analyser can be used to visualise many hours of averaged data and estimate the frequencies which are most active at this site.

- source a spectrum analyser suitable for performing a site survey
- perform the survey at this site
- repeat until suitable site is found
- deploy the antenna at a site

Data Collection

Jupiter is visible above the horizon at night only during certain periods see Figure. 11a on page 16. In order to perform the required data collection it is highly desirable to automate the process if possible.

- create listening schedule during which DAM emissions are likely to occur using the Radio Jove software
- develop SDR prototype mechanism for gathering raw data from the antenna

Data Analysis

Collected data can be analysed manually at first in order to validate the testbed, but later using software such as the development of basic algorithms to spot events such as S-Bursts occurring in the data.

- analyse data collected for evidence of Jovian or Solar DAM emissions

- analyse data for evidence of interference from human sources
- analyse data for evidence of interference from natural sources
- develop a system which connects to the worldwide dxcluster system and creates flag events for human identified emissions at or near the target frequency being monitored by the telescope
- develop a system which interacts with the Blitzortung servers and creates flag events for emissions generated by lightning

Design Platform

An analysis of the current available IoT technologies and some of the available options which could be used in order to produce an open low cost platform which amateur astronomers could use in order to study emissions in the DAM band.

- design a low cost platform suitable for collection of signals to produce power plots or spectrograms in order to identify DAM emissions originating from Jupiter

The SDR hardware transceiver used is likely to be the HackRF system while the SDR software components will be developed in either C++ or Python as both languages have bindings for the GNURadio development tool-kit [Gnuradio, 2014]. The backend aggregation system with API will most likely be developed in the Ruby language as this language is highly expressive and suitable for rapid prototype development. Execution of the Ruby application on the Java VM is capable using the JRuby system, which will also allow the incorporation of any required Java libraries.

Research Questions

The initial research questions which arise are as follows:

1. *What current Internet of Things (IoT) technologies would best suit the development of a software defined radio signal listening station and how cheaply can it be created?*
 - How expensive would a renewable power supply solution such as solar be?
 - Can a low powered computing platform such as the Raspberry Pi B+ suitably host the system, or will a more powerful platform be required?
 - How feasible are wireless technologies such as Zigbee, WIFI or Bluetooth to stream collected data to a central facility?
2. *What processes or algorithms need to be developed to filter or flag known instances of human interference from radio signal observations?*
 - Flag transmission signals identified by amateur radio enthusiasts from a local DXSpider server in recorded data.
 - Flag instances of natural radio interference such as lightning from the Blitzortung server in recorded data.
3. *What SDR tools, processes and or algorithms need to be developed to identify instances of the three main DAM emission types detailed in Table. 1?*
 - Can existing tools and signal processing techniques be employed to find DAM emissions?
 - What is required from an algorithm which might identify DAM emissions within an IQ signal?

Literature Review

The literature review can be broken down into the following areas:

- What are the decametric radio emissions and what are they caused by
- Potential radio telescope designs which could be replicated in order to collect DAM emissions
- Digital signal processing

Decametric Radio Emission: What are they and where do they come from?

[Belcher \[1987\]](#) states that the data collected by both Voyager spacecraft fit with the Alfvén wing theory as an explanation for the source of the DAM emissions [[Belcher, 1987](#)]. [Kivelson et al. \[1996\]](#) discusses the refinements made to this theory to take into account the flowing plasma between Jupiter's ionosphere and the electrically conducting Io. The Galileo spacecraft collected data which appears to corroborate the updates to the Alfvén wing model [[Kivelson et al., 1996](#)]. [Bose et al. \[2008\]](#) states that the Alfvén waves reflect off Jupiter's ionosphere which cause the DAM emissions to radiate out from the point in Jupiter's ionosphere where it meets the IFT in a cone shape. [Imai et al. \[2008\]](#) proposes an update to this model to take into account the decade long shifts in DAM emission patterns, and proposes an extension to the emission cone model to include a searchlight shaped emission zone [[Imai et al., 2008](#)] see Figure. [41](#) on page [64](#).

Radio Telescope Designs: Which to Choose?

The NASA project Radio Jove recommended the dual dipole array design for a cheap low cost listening site as shown in Figure. [12](#) on page [16](#) [[NASA, 2012b](#)]. But it is by no means the only antenna design which would be capable of picking up the DAM emissions. [Wilkinson and Kennewell \[1994\]](#) recommends a slightly more advanced design, the folded dipole which maximises the bandwidth available to the antenna [[Wilkinson and Kennewell, 1994](#)]. [Greef \[2012\]](#) details a third alternative for collecting DAM emissions, a shortwave loop antenna as can be seen in Figures. [43a](#), [43b](#) and [43c](#) on page [65](#).

Digital Signal Processing

[Smith \[2003a\]](#) explains that digital signal processing is a term used to describe the mathematics, algorithms and techniques used to manipulate signals after they have been converted from analogue to digital. [Freidt \[2013\]](#) holds that digital signal processing is the preferred means to process signals, for reasons such as stability and for its resistance to long term ageing effects that analogue systems suffer from. However as [Smith \[2003b\]](#) points out, due to the nature of the conversion from analogue to digital, information is lost in this process. [Smith \[2003b\]](#) maintains that the proper sampling of an analogue signal occurred if you can reconstruct the signal from the digital samples collected, and incorrect sampling will lead to loss of the original signal due to aliasing.

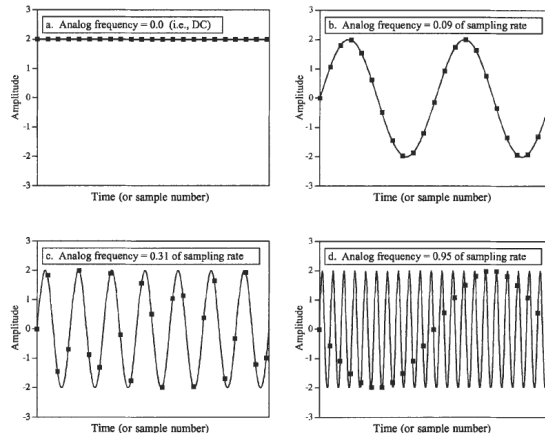


Fig. 13: Sampling an Analogue Signal [[Smith, 2003b](#)]

[Smith \[2003b\]](#) demonstrates in Figure. 13 on page 21 how signal data loss occurs due to aliasing. When sampling an analogue signal which has a frequency more than half of the sample rate (Nyquist frequency), [Smith \[2003b\]](#) observes that the original signal cannot be reconstructed. This is referred to as the sampling theorem [[Smith, 2003b](#)] where f_s is the sample rate and f is the frequency being sampled.

[Ossmann \[2015b\]](#) contends that the application of Nyquist-Shannon sampling theorem only applies to real analogue signals where the bandwidth is equal to

$$f_s > 2f \quad (6)$$

Fig. 14: Sampling Theorem aka Nyquist-Shannon sampling theorem [Smith, 2003b]

half the sample rate. However for a complex digital signal the bandwidth is equal to the sample rate [Ossmann, 2015b].

Due to the cheap availability of computational resources, digital signal processing is capable of being carried out now within software entirely, this has led to the development of software defined radio solutions [Freidt, 2013]. The GNU-Radio software allows creation of software defined radio solutions by replacing hardware functions with modular software functions. These software functions are capable of being connected together, an output from one function providing input for another. It is in this fashion it is possible to transform digital signals using digital signal processing methods within the GNURadio platform[Gnuradio, 2014].

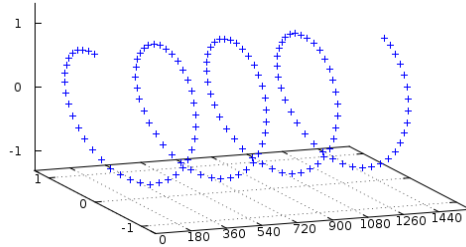


Fig. 15: I/Q Samples Helix [Kuisma, 2014]

Ossmann [2015a] illustrates how the HackRF One SDR transceiver can be accessed within GNURadio by way of the osmocomm source which is an abstraction layer between GNURadio and the HackRF driver. Figure. 45a on page 66 shows an amplitude modulation signal which has been digitally sampled. In order to demodulate such a signal, an understanding how the signal data is stored is a must. Digital periodic signal samples tend to be stored in a complex format which amounts to polar coordinates [Ossmann, 2015c]. I is the point on the real

axis, and Q is an angle which contains the imaginary component. See Figure. 15 on page 22 shows how these I/Q values are plotted periodically and Figure. 16 on page 23 shows the I/Q polar data [Kuisma \[2014\]](#).

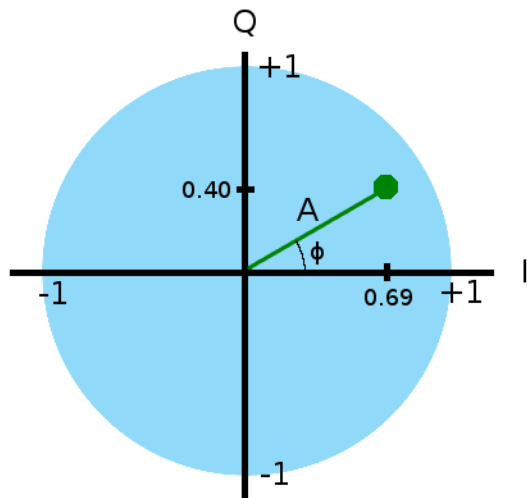


Fig. 16: I/Q Samples Polar Plot [[Kuisma, 2014](#)]

Topic	Belcher 1987	Kivelson et al 1996	Bose et al 2008	Imai et al 2008
What are the Jovian DAM emissions and what causes them?	Large fraction of DAM emissions come from point where IFT meets Jupiter's ionosphere (p3). Large moving conductor within a magnetised plasma (p1) produces Alfvén wing.	Alfvénic disturbances, generated by flowing plasma from Jovian magnetosphere and conducting Io (p337).	Alfvén waves reflecting off Jupiter's Ionosphere (p79).	Not fully understood, but believed to be produced by cyclotron maser instability [Imai et al., 2008].
Topic	Wilkinson et al 1994	NASA Radio Jove 2012	Greef 2012	
Radio telescope designs suitable to capture DAM emissions from Jupiter	Wilkinson et al suggest a folded dipole antenna design	Radio Jove project suggest a dual dipole antenna	Greef demonstrates a low cost Loop Antenna design with reflection plate	
Topic	Smith 2003	Freidt 2013	GNU Radio 2014	Ossmann 2015
Digital signal processing	Smith argues digital signal processing is one of the most powerful technologies that will shape the 21st century.	Freidt states digital signal processing now ubiquitous, and cheap availability of computational power lends self to software defined radio solutions.	GNURadio allows digital signal processing using transformation functions developed in software.	Ossmann argues that the HackRF One is perfectly suited as a low cost wide range transceiver for use within software defined radio prototypes.

Table 2: Literature Review Synthesis Matrix

Testbed Build and Verification

The NASA Radio Jove dual dipole antenna design (Figure. 12 on page 16) was chosen over the other designs for a number of reasons, namely:

- Simplicity of the architecture and consequently also construction
- Low cost of building materials
- Reasonably effective performance (5-9 dB gain depending on configuration)
- Easy to operate and maintain
- Suitable for a permanent installation
- Large body of technical documentation supporting the operation

Special Resources Required

The following resources have been identified as being required in order to perform the research and are listed as follows:

GnuRadio

The GnuRadio software is an open-source software development tool kit that allows access to signal processing techniques in order to implement software radio solutions.

HackRF

The HackRF SDR transceiver system is the software defined radio transceiver chosen for the prototype system.

PL259 / SO239

Cable adapters which connect coax cables together with the dipole centre.

Radio Jove Software

The Radio Jove software is extremely useful for observers wishing to capture DAM emissions from Jupiter. It contains a large number of features such as emission prediction observation charts, and information regarding Jupiter's location in the sky from any specified point on the Earth's surface.

RG59 Coax

RG59 coax cable is required to link the dipole antennas back to the SDR transceiver.

Spectrum Analyser

A spectrum analyser will be required in order to perform a site survey to determine if a location is suitable for collecting DAM emissions.

Antenna Build

In order to satisfy the main requirement of capturing DAM signals at 20.1MHz construction of an antenna was needed. The equation shown in Figure. 8 on page 13 was used to calculate a starting estimate of the length of antenna wire required to construct this antenna. Many factors can affect the ability of an antenna to receive data at a particular frequency [ARRL, 2000], such as the following:

- quality of the wire conductor or thickness of the wire
- height that the antenna is mounted above the ground
- capacitive end effects
- closeness to radio conductors

One simple method of partly improving antenna performance is by controlling the length of the antenna wire while measuring the Standing Wave Ratio (SWR) value, which is the ratio of the maximum peak voltage anywhere on a line to the minimum value at any point along the same line. The use of a SWR analyser becomes invaluable in this process.



Fig. 17: Measuring the SWR of the antenna with an SWR Analyser

The initial length of antenna wire was cut to match the length produced by the equation in Figure. 8 on page 13 and was then cut in half before each end was connected to a dipole centre. The antenna was placed on the ground before being connected to the SWR analyser. The SWR value for the antenna was measured, and it was discovered the antenna was suitable for capturing of signals at 18 MHz. The antenna was then shortened by a small identical amount on each side

and the SWR values were again measured until the antenna registered as being most suitable for operation at 20.1 MHz as seen in Figure. 17 on page 26.

The SWR equations shown in Figure. 18 on page 27 $|\rho|$ is the reflection coefficient, P_f is the power in the forward wave entering the antenna while P_r is the power of the reflected wave in the antenna [ARRL, 2000].

$$SWR = \frac{1 + |\rho|}{1 - |\rho|} \quad (7)$$

$$|\rho| = \frac{SWR - 1}{SWR + 1} \quad (8)$$

$$|\rho| = \sqrt{\frac{P_r}{P_f}} \quad (9)$$

Fig. 18: Standing Wave Ratio Equations

$$|\rho| = \frac{1.2 - 1}{1.2 + 1} \quad (10)$$

$$|\rho| = 0.0909090909090909088 \quad (11)$$

$$0.0909090909090909088 = \sqrt{\frac{P_r}{100}} \quad (12)$$

$$0.0909090909090909088^2 = \frac{P_r}{100} \quad (13)$$

$$P_r = 0.826446280991735 \quad (14)$$

Fig. 19: Calculating P_r for the antenna

The value of SWR for the antenna should be ideally as close as possible to 1, this ensures all the signal energy collected by the antenna is transferred to the load successfully. However in practice this is never the case as all antennas have varying amounts of loss. The antenna once mounted had a measured SWR value of 1.2 which equates to a P_r value as shown in Figure. 19 on page 27 of 0.826446280991735 which is a loss of 17.35% or about 1 dB which is considered reasonable [ARRL, 2000].

Table: 3 gives a breakdown of the costs associated with the antenna build to date. While Table: 4 gives the breakdown of the official NASA Radio Jove kit for comparison.

Item Name	Cost (€)
100m Copper Wire	20.00
100m Coax RG59	25.00
2 × Dipole Centers	20.00
8 × PL259	18.00
2 × SO239	4.00
SMA-SO239 Adapter	4.50
2 × SO239-SO239 Adapter	4.50
T Adapter	3.00
Patch Lead	5.00
2 × 4m 5cm Pipe	15.00
2 × 4m 4cm Pipe	15.00
HackRF Transceiver	315.00
RTL DAB Receiver	25.00
MCX-SO239 Adapter	6.50
Total	480.00

Table 3: SDRT Build Cost

Item Name	Cost (€)
RF 2080 Calibrator/Filter	100.00
Receiver	295.00
Antenna Kit	65.00
International shipping	60.00
Total	520.00

Table 4: SDRT Build Cost [[NASA, 2014](#)]

Listening Site Suitability

A convenient location for the antenna deployment was selected and the antenna was deployed. It was necessary to determine if this site was in fact a suitable location to host a radio telescope antenna. In order measure the ambient noise at the site, a Tektronics SA2600 spectrum analyser was connected to the antenna and left for 2 hours at midday to gather data. The spectrum is likely to be full of radio interference from human and natural sources at this time. The results can be seen in Figure. 20b on page 30. The ambient RF noise at the site was quite high, ranging between -80 dB and -70 dB on average.

Similar readings were taken using the HackRF while attached to the antenna as show in Figure. 20c on page 30. The measurements recorded with the HackRF were performed using the *gqrx* SDR software while all amplification settings inside *gqrx* were set at 0, in order to get an accurate reading on the raw signal being collected by the antenna. The values were on average -20 dB quieter than those recorded by the SA2600 spectrum analyser, this points towards an inherent deafness flaw in the HackRF design itself, and possibly the requirement of a pre-amplifier (preamplifier) in order to boost the gain on the input signal.

In May 2013, the Solar Physics Group from Trinity College Dublin, performed a site survey at Birr Castle to ascertain the suitability of the site for an installation of the Low Frequency Array (LOFAR) telescope [[McCauley, 2013](#)]. The study was focused on a wide range of frequencies between 10 and 400 MHz, a portion of which can be seen in Figure. 20d on page 30. The report concluded that the location at Birr Castle was a relatively quiet location as compared against a site at Bornim, Germany and another at Bleien, Switzerland.

From the results of this survey, it can be seen that the average background noise levels were about -55dB near 20 MHz which is similar to those recorded

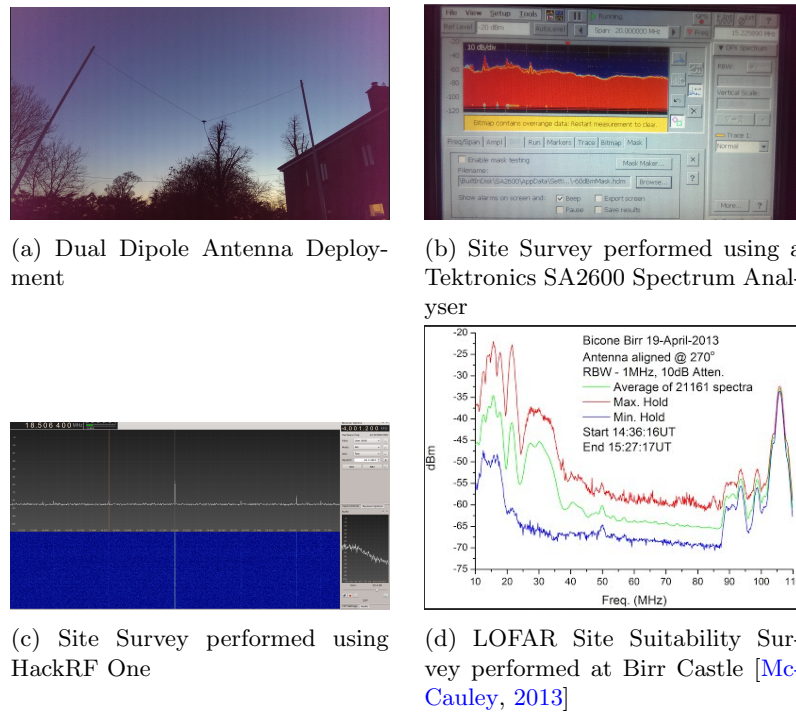


Fig. 20: Site Survey

80 km away at the Kilkenny site. Table: 5 details the results collected at the Kilkenny site and includes those performed by the Solar Physics Group at Birr Castle for comparison. Results indicate the Kilkenny site appears to be a reasonable location at which to host the radio telescope.

Site	Equipment	Average Noise at 20.1 MHz
Kilkenny	Tektronix SA2600 20.1 MHz Dipole	-65 dB
Kilkenny	HackRF One 20.1 MHz Dipole	-65 dB
Birr	LOFAR Array 10-100 MHz Schwarbeck Bicone	-55 dB

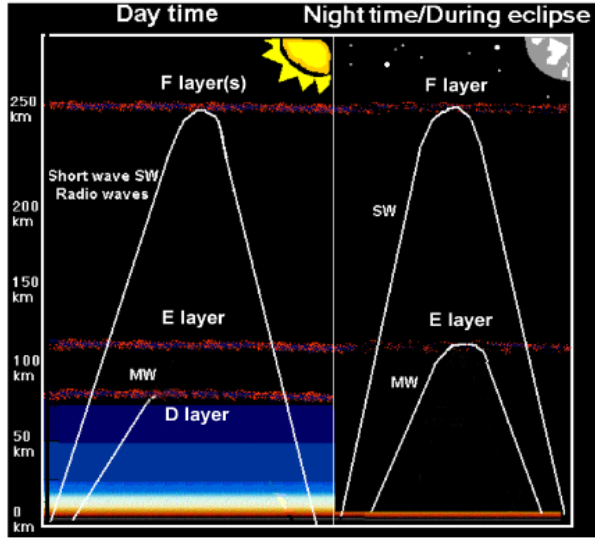
Table 5: Average Noise Measurements at Kilkenny Listening Site compared to Birr Listening Site [McCauley, 2013]

Verification of the Radio Receiver

An opportunity to validate the HackRF transceiver arose with the announcement of a public Medium Wave (MW) experiment by [Nichols \[2015a\]](#) of the Radio Society of Great Britain (RSGB). The RSGB Propagation Studies Committee intended to perform an experiment during the partial solar eclipse on 20th March 2015. As can be seen in Figure. 46 on page 30, the UK and Ireland would witness more than 90% totality during the eclipse. This was an opportunity to perform simple experiments to demonstrate the Sun's effect on Earth's ionosphere, and how this ionisation affects the propagation of radio signals.

According to [Nichols \[2015b\]](#), MW radio stations which are located more than 500 km away are unlikely to be propagated during daylight hours due to their signals being absorbed by the D layer as shown in Figure. 21 on page 32. However this D layer does not exist during night time hours, as a result these radio signals are free to reflect from the E and F layers. [Nichols \[2015a\]](#) states that this is also true during a solar eclipse with a high totality percentage as would occur on the 20th March 2015.

[Nichols \[2015a\]](#) provided some a number of radio stations which transmit signals in the MW range at various locations in the United Kingdom, Europe and also a number in Iceland. The experiment called for choosing a station which is transmitting in the MW range and is capable of being heard at the listeners location during the night time. This station should not be capable of being heard



How medium wave (MF, 300 kHz to 3 MHz) and short wave (SW, 3-30 MHz) radio waves can be reflected/refracted from the different layers of the ionosphere during the day and during an eclipse or at night.

Fig. 21: Comparing propagation of MW radio signals during day and during night/solar eclipse [Nichols, 2015a]

during the day time, the experiment called for a station which is further away than 500 km. The chosen radio station should then be tuned in to coincide with the beginning of the solar eclipse. The station receive power should be plotted against time. It was expected that the signal strength of the radio station should rise to a maximum which coincided with the solar eclipse maximum.

It was immediately apparent that the Radio Jove antenna design would not be suitable for this experiment, and a suitable alternative was examined. During the initial research into potential designs a paper by Litva and Rook [1976] mentioned the use of a Beverage antenna for use in highly directional receivers such as early transatlantic radio communication experiments. Due to the simple nature of the Beverage antenna design, this was considered for use in this experiment.

Methodology

The following methodology was followed during this experiment:

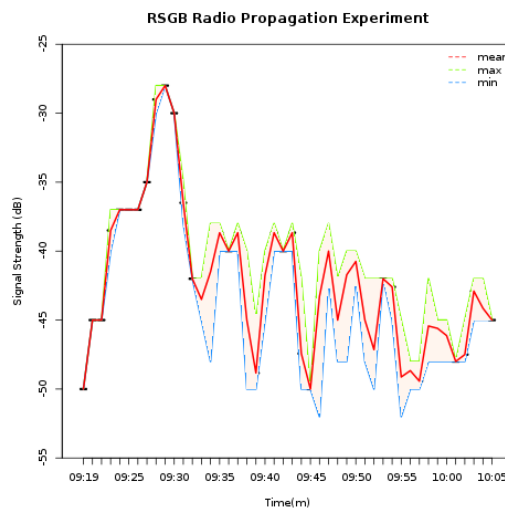
1. The dipole antenna built for use in the main part of the dissertation was not best suited for picking up signals in the MW range so an alternative design was chosen.
2. A Beverage antenna was picked as it was easily aimed and had a simple design. The antenna very simply consisted of a copper wire 80 m long attached to a long wire antenna terminator which had an SO239 connector [[Litva and Rook, 1976](#)].
3. The listening site was longest in the East-West axis, and having the receiver positioned at the far west end of the site was most convenient. For this reason a radio station situation in an Easterly direction was picked.
4. The antenna was aimed in the general direction of the radio station chosen, and simply placed on the ground.
5. HackRF was tuned to the chosen radio station.
6. 2 MHz bandwidth of the spectrum was recorded during the entire length of the solar eclipse, the signal strength of the radio station can be plotted against time at a later date using this recorded data.
7. The SDR receiver should have the automatic gain control switch off in order to get accurate power results.

The chosen radio station was *Radio China International* (1.440 MHz) which was a powerful signal during the night time despite it being transmitted from Marnach in Luxembourg which is *distance* $\approx 950\text{km}$ away from the listening site. Once the solar eclipse began, the HackRF SDR receiver was tuned to 1.440 MHz with a bandwidth of 2 MHz and IQ samples were recorded. As the eclipse neared 20% totality, the radio station began to emerge from the background noise at -55 dB. The signal rose steadily until the eclipse maximum point which was -28 dB, and then averaged at a level of -45 dB as the totality value dropped. At 20% of eclipse totality, the station faded once more before disappearing into the background noise level at -55 dB. The results were plotted in Figure. [22a](#) on page [35](#) and were submitted to [Nichols \[2015a\]](#) for inclusion in the overall experiment.

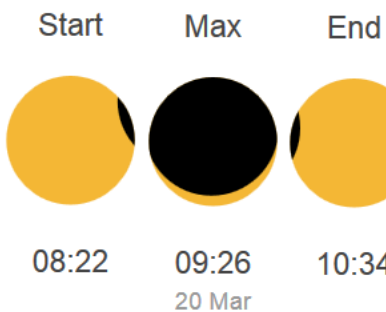
A number of issues with the HackRF SDR transceiver were discovered during this experiment. The technical specifications show the operating range of the HackRF to be 10 MHz - 6 GHz [[Ossmann, 2015d](#)]. In practice it possible to tune to frequencies below 4 MHz, even as low as 500 kHz with a few caveats.

Reliable tuning proved a problem below 10 MHz, when the HackRF was power cycled, tuning to the same frequency in software would see the station vanish. It took trial and error to find it once more by scanning lower and higher until the station was reacquired. This is due to the internal signal oscillator being affected by many external variables such as temperature. To be certain of the exact frequency being monitored, an external clock source must be used to provide a signal reference to the system.

The HackRF also appears to be quite deaf without maxing the IF and RF amplifiers. This could be solved by adding a preamp and a bandpass filter between the antenna and the receiver. An example being the RF-2080 C/F device which has been designed specifically for capturing DAM emissions from Jupiter [NASA, 2010]. The RF-2080 device, contains a 25,000 K noise source and a bandpass filter which allows signals at 20.1 MHz through to the receiver while reducing the interference from large radio stations near this frequency.



(a) Plot of signal power vs time



(b) Solar eclipse totality progress

Fig. 22: 20th March 2015 solar eclipse

Capturing DAM Emissions

Using the Radio Jupiter Pro software, a prediction was made that 23rd April 2015 would offer a very good opportunity to hear DAM emissions. As can be seen in Figure. [23a](#) on page [37](#), at the point of the highest chance of capturing DAM emissions, Jupiter was right on the very edge of the antenna beam focus. Due to the limitations in the design of the antenna, this configuration offered the best chance to receive an emission from Jupiter.

Despite this, a number of emissions were recorded as can be seen in the raw image Figure. [23b](#) on page [37](#). The emissions appear as faint horizontal lines in this waterfall diagram. This diagram is limited by the small bandwidth of 2 MHz and short period of 2 minutes. Ideally in order to spot these interesting emissions a large bandwidth of 20 MHz for instance should be used, over a long period of observation such as 1-24 hours. An example of this is section of a spectrogram seen in Figure. [23c](#) on page [37](#), which shows averaged signal power data for frequencies 17-55 MHz and 70-1000 MHz for a 24 hour period.

There are many open source software tools such as `rtl_power`, `simple_ra` and `heatmap.py` which could capture averaged raw signal strength data from a RTL based receiver in order to build spectrogram diagrams. Unfortunately most of this software is not compatible with the HackRF. However the basic functionality from these tools can be replicated using basic processing blocks within GNURadio and the spectrograms can be built using tools like Octave or Matlab.

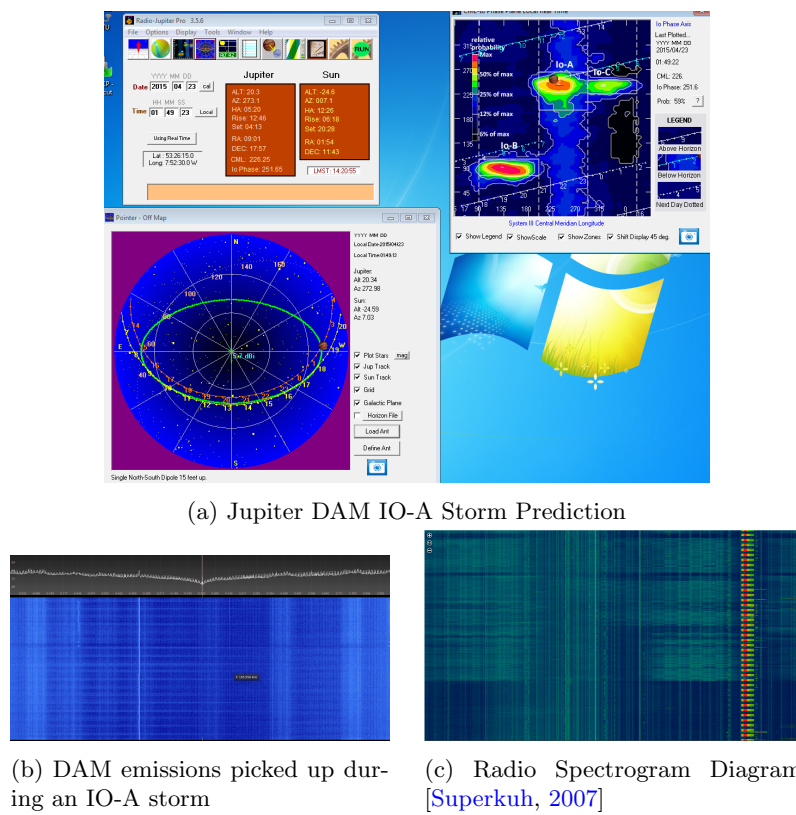


Fig. 23: DAM Emissions

Research Question 1

What current Internet of Things (IoT) technologies would best suit the development of a software defined radio signal listening station and how cheaply can it be created?

- How expensive would a renewable power supply solution such as solar be?
- Can a low powered computing platform such as the Raspberry Pi B+ suitably host the system, or will a more powerful platform be required?
- How feasible are wireless technologies such as Zigbee, WIFI or Bluetooth to stream collected data to a central facility?

Determine SDRT Power Requirements

A major component of designing a self sufficient system is choosing the power supply. One solution is the use of renewable sources such as wind or solar to generate power and the use of batteries to act as a buffer and storage of this energy. When a suitably large battery array is deployed, power to the system can be provided during periods when there is no sunshine or wind available.

In order to design a self sufficient listening site it was necessary to firstly determine the power requirements of the hardware essential to the functioning of the system. If there are high computational requirements the system will generally also have high power needs, which can have a drastic effect on the cost of implementing a sustainable power supply using renewables. It is prudent therefore to implement the system as cheaply as possible, and using low powered devices.

The SDR RTL and HackRF receivers require a minimum of a USB 2.0 interface and computational requirements for processing data which immediately reduced the potential platforms to devices such as the Raspberry Pi B+, Raspberry Pi B2 and the Intel Atom or better.

Methodology

The following platforms were chosen for testing purposes as they initially appear to meet or exceed the minimum requirements of operating rtl_power while also building spectrograms from the recorded data using heatmap.py:

1. Raspberry Pi B+ 800MHz, 512MB RAM
2. Raspberry Pi B 2. 900MHz, 1GB RAM
3. EEEPC Intel Atom N550 Netbook. 1.55GHz, 2GB RAM

Each platform would be tested on the following metrics:

Idle

The power usage while the system is at rest

heatmap.py

The power usage while the system is building spectrogram with heatmap.py

rtl_power

The power usage while the system is collecting data with rtl_power

Both heatmap.py and rtl_power

The power usage while the system is building spectrogram with heatmap.py and collecting data with rtl_power

100% CPU Load

The power usage while the system is at 100% load

The power usage of each system was measured using a power meter and the results were plotted as shown in Figures. [24a](#), [24b](#), and [24c](#) on page [40](#).

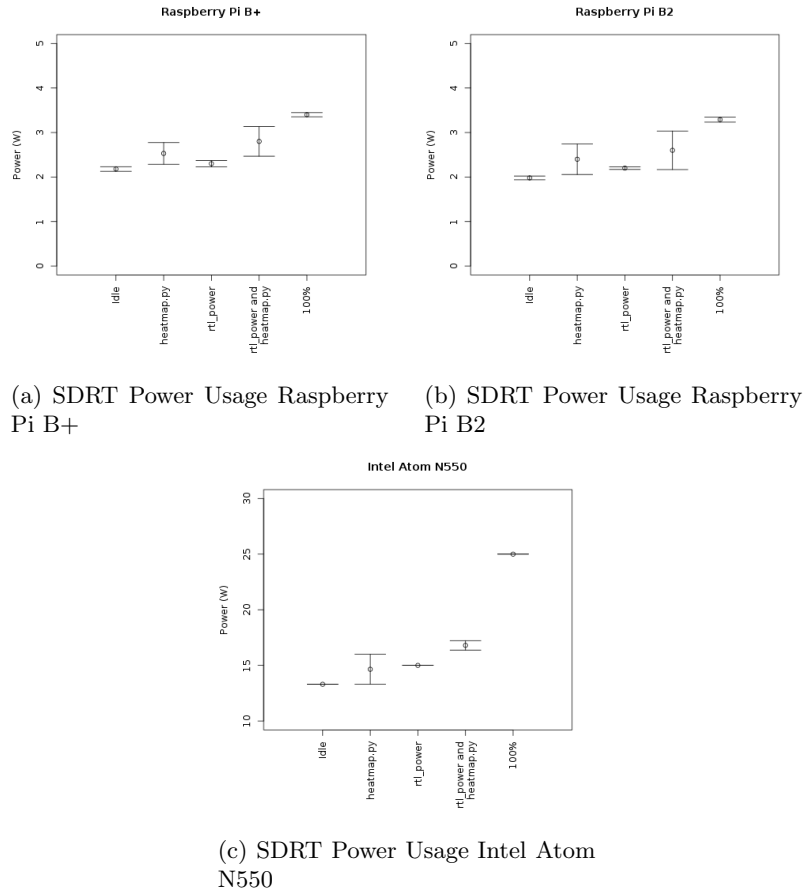


Fig. 24: DAM Emissions

Using solar data collected by the national weather service, MET Eireann [MET, 2015] and [ECA&D, 2015], a period between 1961 and 1977 of solar data was averaged in order to create a series of plots to aid in the calculation of the battery array capacity required to power the system. As can be seen in the Figure. 27b on page 43, the mean number of hours of sunlight for this period of time was calculated to be $\mu = 4.446$, with a minimum of 1 hour and a maximum of 9.156 hours.

$$\text{Power(Watts)} = \text{Current(Ampere)} \times \text{Voltage(V)} \quad (15)$$

$$A = \frac{W}{V} \quad (16)$$

$$A = \frac{25}{12} \quad (17)$$

$$\text{Ampere} = 2.08333333A \quad (18)$$

Fig. 25: Calculating Amps using Watts and Voltage

Consumer solar panels generally operate at voltages between 12 - 48 V, and should when coupled with a battery charge controller, ensure a battery bank which may be operating on a lower voltage, can be safely recharged using generated power [Bryce, 2011]. The load power value measured previously for the Intel N550 Netbook operating at 100% was 25 W. Taking the load and the assumed voltage value of 12 V, the load current was generated using the power equation shown in Equation: 25. The current required to generate 25 W at 12 V is 2.0833333 A.

An initial estimate of 48 hours of power capacity was made to ensure the system can be powered for an extended period during periods of low solar activity. A plot of load vs battery capacity was generated as shown in Figure. 27a on page 43. This plot shows the capacity value required to satisfy a 25 W load at 12 V for a 48 hour period is about 100 Ah. When using lead-acid batteries, it is wise never to consume more than 20% of capacity, otherwise unnecessary degradation of the battery will occur [Bryce, 2011]. For this reason to safely consume 100 Ah, the battery bank total capacity should be closer to 500 Ah.

Figure. 27b on page 43 shows the averaged daily hours of sunshine over a 15 year period. This plot demonstrates that for half the year the sun shines for

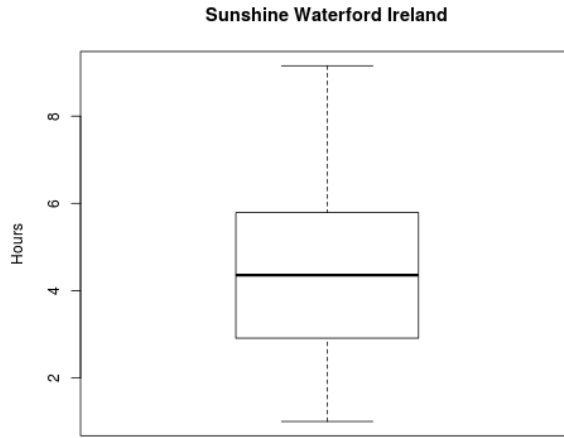


Fig. 26: Average Daily Sunshine in Waterford

between 1 and 4 hours each day. This is a major limiting factor in creating a self sufficient solar powered system, as batteries may only be charged during periods of sunshine. During the times of the year with daily sunshine hours below the mean, a larger battery capacity is required in order to continue to power the system during days with little sunshine. Correspondingly, as the sunshine hours fall, a larger solar panel is required to ensure as much light as possible is converted to energy storage.

Next a plot of solar panel power output vs time taken to charge a 500 Ah battery was generated as Figure. 27c on page 43. This plot shows that in order to reliably charge a battery of size 500 Ah in a single day which has the mean hours of sunshine the system will require a solar panel array of at least 2.5 kW.

The measurements were repeated for the Raspberry Pi systems. The power demands were rounded up to 5 W which produced a battery capacity of 80 Ah to power for 48 hours. The results were then tabulated as shown in Table: 6. The components required to implement a solar powered system such as the panels, batteries, charge controller and AC/DC inverters were priced and the results were included in this table also. Price wise, having a Raspberry Pi system in the listening station would make for a cost effective solution. As both the B+

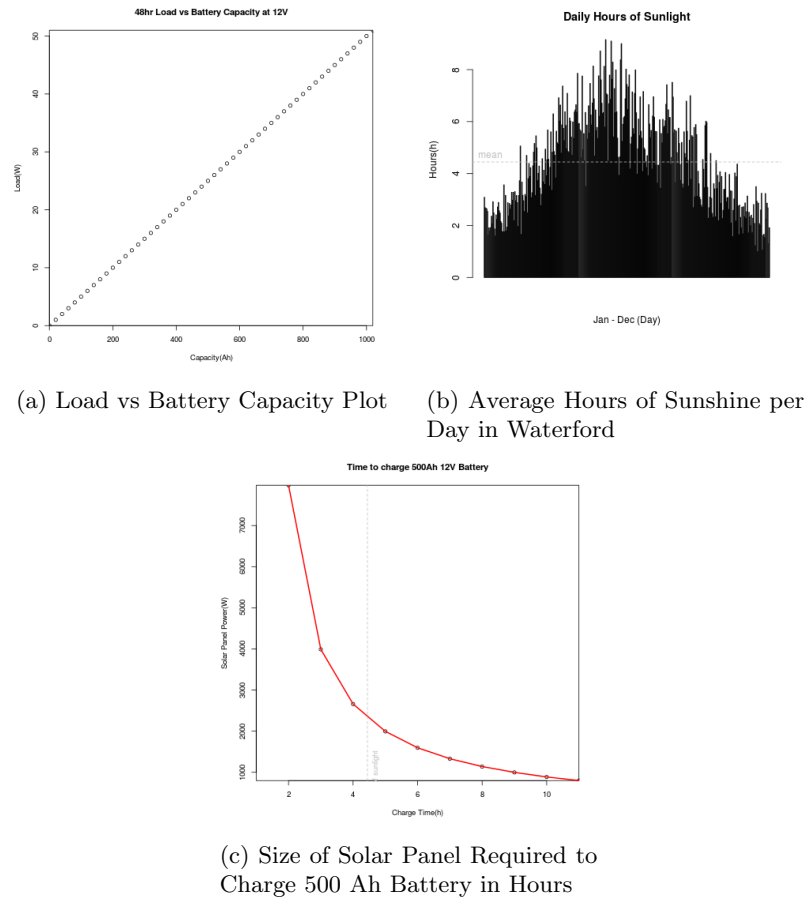


Fig. 27: Solar Plots

and the B2 versions operate with the very low power usage of 5 W, the solar renewable solution would be cheapest also at an estimated €300 for the solar power components.

Equipment	Solar Panel Power(W)	Battery Capacity(Ah)	Estimated Cost(€)
Raspberry Pi B+	330	80	300
Raspberry Pi B2	330	80	300
Intel Atom N550	2500	500	2500+

Table 6: System Power Requirements

Determine SDRT Computational Power Requirements

The aim of this experiment was to determine the minimal hardware which was computationally capable of collecting data, while performing any data analytical or processing tasks required by the system.

Methodology

The following platforms were chosen for testing purposes as they initially appear to meet or exceed the minimum requirements of operating `rtl_power` while also building spectrograms from the recorded data using `heatmap.py`:

1. Raspberry Pi B+.
2. Raspberry Pi B 2.
3. EEEPC Intel Atom N550 Netbook.
4. Intel i5-3340M 2.7GHz

Each platform would be measured under a single metric, namely the length of time it takes to produce a spectrogram from data collected over a 24 hour period. Table: 7 shows the results gathered on each platform. As the time taken to process the spectrogram was longer than 24 hours for both Raspberry Pi models tested, they could not be considered capable of hosting the SDRT system and so this particular test was aborted when the time exceeded 24 hours for both Pi models.

The Intel Atom powered Netbook performed considerably better with a result of 4.12 hours. This would allow the collection of data, while also the sustainable processing of the previous days data without becoming overloaded.

Equipment	Generate Spectrogram(h)
Raspberry Pi B+ 800MHz 1 Core	24Hrs+
Raspberry Pi B2 900MHz 4 Core	24Hrs+
Intel Atom N550 1.55GHz 2 Core	4.12hours
Intel i5-3340M 2.7GHz 2 Core	0.25hours

Table 7: System CPU Power Requirements

Determine SDRT Network Connectivity Requirements

The aim of this experiment was to determine the optimal networking technology to transfer collected and or processed data from the SDRT to another system.

Methodology

The following technologies were investigated during this experiment:

1. Zigbee (XBEE Pro 2B 802.15.4)
2. WIFI (802.11N)
3. Fast Ethernet (802.3u)
4. Gigabit Ethernet (802.3-2008)

Each technology was measured using a single metric, transfer speed to copy 2GB of collected data between two nodes in the network. Table: 8 shows the results obtained.

There existed a large discrepancy between the estimated values and the actual measurements obtained for several technologies measured. A number of factors could account for this, such as the estimated values being generated using theoretical maximum bandwidth for the technology, which are unrealistic for real world applications.

One example is the underlying hardware which handles both the USB and the Fast Ethernet network interfaces on the Raspberry Pi systems has a limit of

Technology	Bitrate	Est(s)	Result(s)
Zigbee	250kbit/s	76,000	24Hrs+
WIFI N	144Mbit/s	132	737
Fast Ethernet	100Mbit/s	181	904
Gigabit Ethernet	1Gbit/s	30	45

Table 8: Networking technologies transferring 2GB data

2Mbit/s, and could therefore never reach the theoretical maximum of 11Mbit/s suggested by Fast Ethernet. Using the Zigbee XBEE 802.15.4 modules, the theoretical estimate of 250kbit/s suggested a time of 21 hours to transfer 2GB of data, however after 24 hours the transfer was still ongoing. As the ability to the collected data must be faster than the time taken to collect it, the Zigbee test was cancelled after 24 hours. The results show WIFI, and Ethernet technologies being preferable in this instance.

Research Question 2

What processes or algorithms need to be developed to filter or flag known instances of human interference from radio signal observations?

- Flag transmission signals identified by amateur radio enthusiasts from a local DXSpider server in recorded data.
- Flag instances of natural radio interference such as lightning from the Blitzortung server in recorded data.

Flag Amateur Radio Enthusiast Transmissions

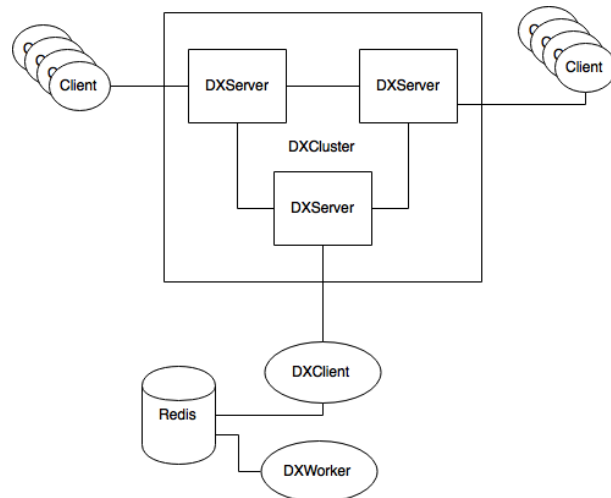


Fig. 28: DXCluster Client Architecture

A DX server is a system which Amateur (Ham) Radio operators may use in order to inform one another in real time, about instances of radio signal transmissions from DX stations and other amateur radio stations. These DX Servers are often connected together to form a cluster. This allows many users from all over the world to communicate and share this information by connecting to the cluster. It is a rich source of identified human transmissions which often

have the time, location and signal frequencies which were recorded. The data being shared is also often rigidly structured which greatly simplifies the task of implementing a software parsing solution [Koopman, 2007]. Table: 9 details the format of each packet of information shared on the DXCluster.

Key	Sample Value
Call Sign of Spotter	DX de EA1MX:
Frequency	144364.0
DX Call Sign	TM64TDF
Comment	IN73XK<TR>IN93OA tnx qso
Time	1623Z

Table 9: Sample DXSpider Data Packet

A software client was developed in order to connect to a local server within the DXCluster. The architecture diagram is shown in Figure. 28 on page 47. It was designed to gather all data from the cluster while filtering transmissions outside the frequency range currently being monitored by the telescope, and also filtering transmissions outside Europe. All signals which have been identified as being within the range being monitored, would be flagged and all related meta data for each transmission would be stored for processing at a later stage.

Methodology

The aim of this experiment was to record 24 hours worth of data on the DXCluster for signals originating in Europe within the frequency range being monitored by the SDRT system. The following methodology was followed during this experiment:

1. Collect 24 hours worth of data using the DXCluster Client developed
2. Filter out all signals not originating in Europe
3. Filter out all signals outside the target range of 18 MHz - 40 MHz

The experiment was run for 24 hours, and during this time, 1984 transmissions were recorded on the DXCluster. The data was filtered to only save transmissions originating from European countries, and also filtered further to only contain transmissions within the range being monitored by the SDRT namely

18 MHz - 40 MHz. This reduced the number of transmissions recorded to 209. The Figure. 29a on page 49 shows a high level breakdown of the most popular countries for which transmissions originated from during the 24 hour period of monitoring. Figure. 29b on page 49 shows this same data broken down by the hour it was collected and finally Figure. 29c on page 49 shows this data broken down by the radio frequency on which the transmission originated. As Figure. 29c on page 49 demonstrates, the majority of signals appear within narrow bands as is to be expected, as amateur radio enthusiasts operate in bands such as the 10 m band for instance which corresponds with a frequency range of 28.000 MHz - 29.700 MHz, and then within channels inside this range.

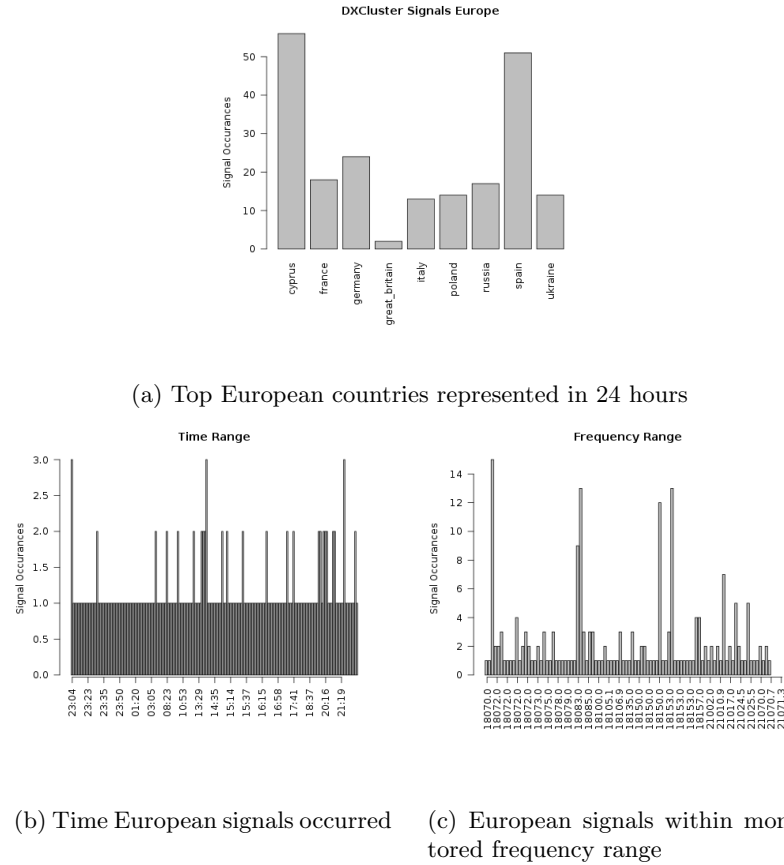


Fig. 29: DXCluster data

Flag Natural Emission Sources

The Blitzortung project operates an online service which displays global information about instances of lightning strikes in real time. [Wanke et al. \[2014\]](#) provide the designs for a listening station which amateur enthusiasts can then build and operate. Each site can share information collected on local instances of lightning with the central server in real time [[Wanke et al., 2014](#)]. A software client was developed which can retrieve data on lightning strike occurrences from within Europe in 10 minute blocks from the Blitzortung server. Table: [10](#) details the format of each Blitzortung data packet.

Key	Sample Value
Date	2015-08-03
Time	21:40:03.600511018
Latitude, Longitude,	
Elevation	pos;43.899106;20.438919;0
Unknown	str;0
Station ID	dev;14497
Confirming Stations	sta;11;24;951,956,1313,1171,803

Table 10: Sample Blitzortung Data Packet

The Haversine function shown in Figure. [30](#) on page [51](#) provides the means to determine the distance between two points on a spherical surface, which Earth approximately is [[Pineda-Krch, 2010](#)]. In this function, φ corresponds with latitude, λ corresponds with longitude and R is the radius of the Earth. This function is used to measure the distance between the location of the SDRT listening site and each individual lightning strike data point. With this distance value, it is then possible to discard data points which originate further from the SDRT listening site than a chosen value such as 1000km.

Methodology

The following methodology was followed during this experiment:

1. Collect 10 minutes of data using the Blitzortung Client developed
2. Filter out all lightning strikes not originating in Europe
3. Filter out all lightning strikes outside the target range of 1000km

$$a = \sin^2\left(\frac{\Delta\varphi}{2}\right) + \cos(\varphi_1) \times \cos(\varphi_2) \times \sin^2\left(\frac{\Delta\lambda}{2}\right) \quad (19)$$

$$c = 2\arcsin(\min(1, \sqrt{a})) \quad (20)$$

$$distance = R \times c \quad (21)$$

Fig. 30: Haversine Formula

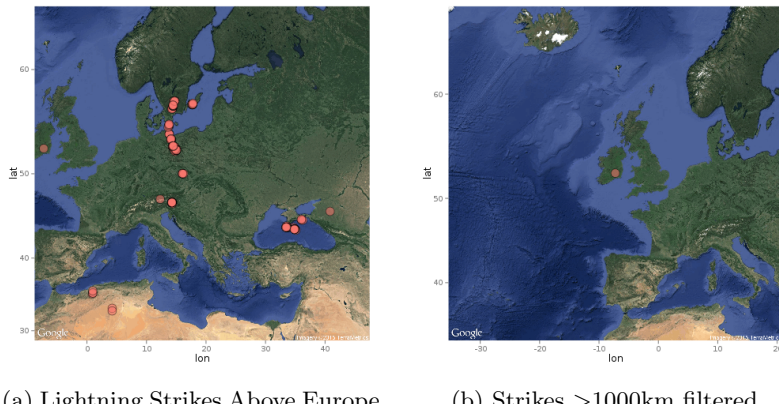


Fig. 31: Blitzortung data

Research Question 3

What SDR tools, processes and or algorithms need to be developed to identify instances of the three main DAM emission types detailed in Table. 1?

- Can existing tools and signal processing techniques be employed to find DAM emissions?
- What is required from an algorithm which might identify DAM emissions within an IQ signal?

Capturing DAM Emissions with the RTL2832 DAB SDR

The Radio Jupiter Pro tool was used to choose a date which was optimal for capturing DAM emissions. The Figure. 32a on page 54, was generated by taking a screen capture of the GQRX tool while connected to the HackRF SDR transceiver. The data was recorded at a bandwidth of 3 MHz for an estimated 2 minutes. The multiple short wide bandwidth bursts are possibly instances of Jovian storm L-Bursts. This spectrogram is a very narrow window considering the capabilities of the HackRF device which has a maximum bandwidth of 20 MHz. Unfortunately the HackRF is limited by the USB transfer speeds of the host computer, and the observations were recorded on a machine with USB 2.0, which prevented data being collected at larger bandwidths. Being limited to 2 minutes per screen capture is potentially of little value in hunting for DAM emissions, as Jovian storms may occur over several hours. Ideally a spectrogram plot generated from 24 hours worth of data is required.

Due to its recent release there is currently no tools available which are capable of interfacing with the HackRF SDR transceiver in order to generate a spectrogram plot from saved data. This speed limitation along with the lack of tooling, raised the possibility of using other devices. The first option being the RTL line of DAB TV receivers which are known to make reasonable SDR receivers, and have a wide selection of tooling already developed. The rtl_power utility is shipped with the firmware required to operate the SDR receiver and is capable of collecting power data over long periods of time with the view to generate spectrogram plots at a later point. One such tool is the heatmap.py utility which is designed to take the output from rtl_power and produce very

large bandwidth and long period spectrogram plots [Keen, 2015]. This was ideal for the purpose of hunting for DAM emissions.

The RTL based receivers have a similar operating range to the HackRF and align somewhat closely with the requirements to pick up DAM emissions from Jupiter [Hamradio-Science, 2012]. Table: 11 lists the operating ranges of both the HackRF and also the RTL DAB receiver. The RTL DAB receiver operates at 24 MHz at the lower end of its operational range. This is still well within the 7 MHz - 40 MHz range of Jovian DAM emissions, but it is just outside the ideal range recommended by NASA's Radio Jove documentation of 20.1 MHz [NASA, 2012b]. The RTL device has a narrow maximum bandwidth of 2 MHz, however this is potentially not such an issue, as `rtl-power` is designed to quickly retune the receiver and take a power reading to enable the sampling of large bandwidths. The retuning of the RTL receiver in order to take a power sample is not instant. It can take several seconds to take a single reading for a large bandwidth so this should be taken into account [Keen, 2015].

Device	Operating Range
HackRF	1 MHz - 6 GHz
RTL2832U/R820T	24 - 1850 MHz
SDRT	7 MHz - 40 MHz

Table 11: RTL vs HackRF and SDRT Requirements

Methodology

The following methodology was followed during this experiment:

1. RTL2832U/R820T Dongle connected to the 21 MHz Dual Dipole Array
2. `rtl-power` was left running for 24 hours at a time recording data
3. A spectrogram was generated using the `heatmap.py` utility from data collected in the previous 24 hours

The plots shown in Figures. 32 and 33 on pages 54 and 55 show possible instances of DAM emissions captured using the RTL receiver over extended recording sessions of 24 hours. In Figures. 32c and 32d on pages 54 and 54, it is possible to see the interference from amateur radio signals while Figure. 33

on page 55 also show the extra noise and interference generated by the Sun when it is above the horizon and crosses into the antenna beam. Using both the `rtl_power` and `heatmap.py` utilities, it seems feasible to capture DAM emissions on a spectrogram.

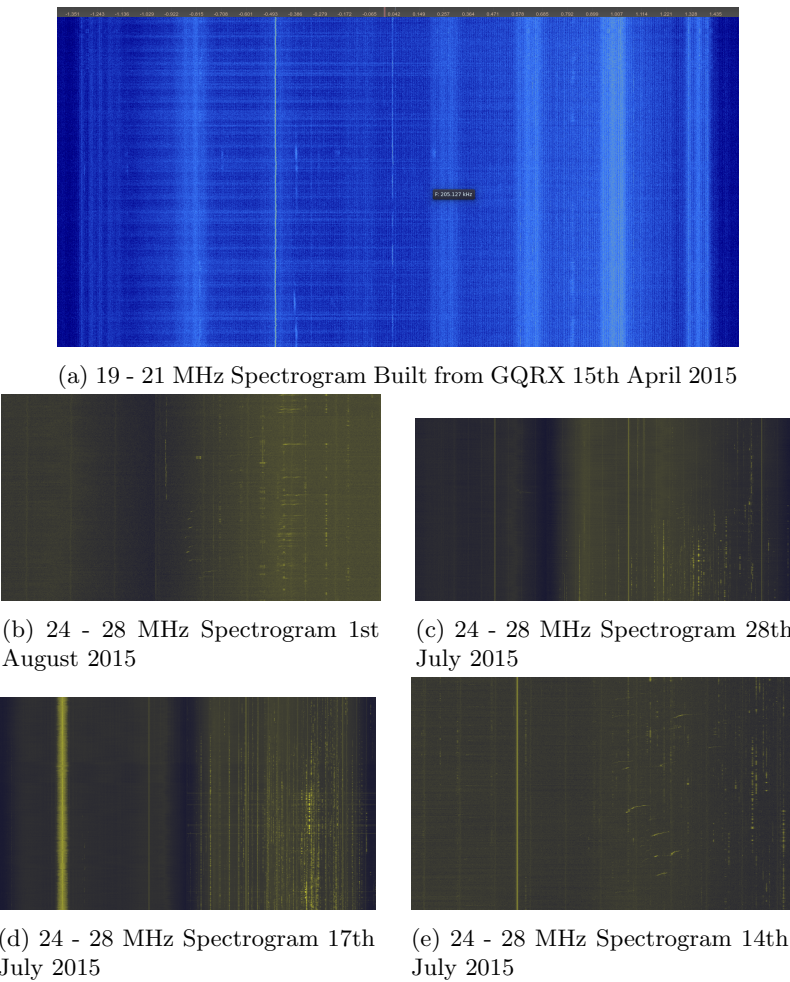
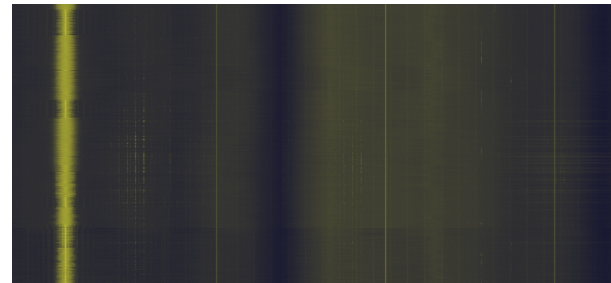
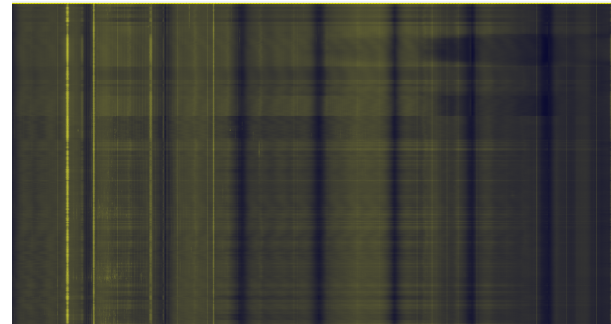


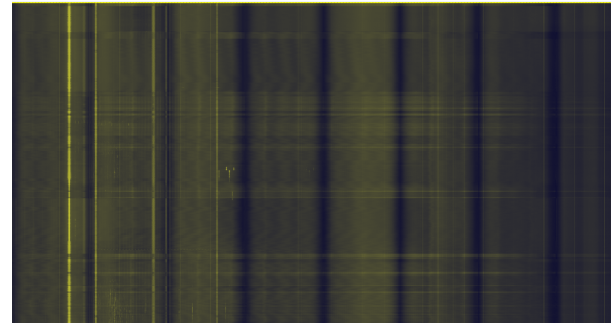
Fig. 32: 24 - 28 MHz Spectrograms of `rtl_power` data plotted using `heatmap.py`



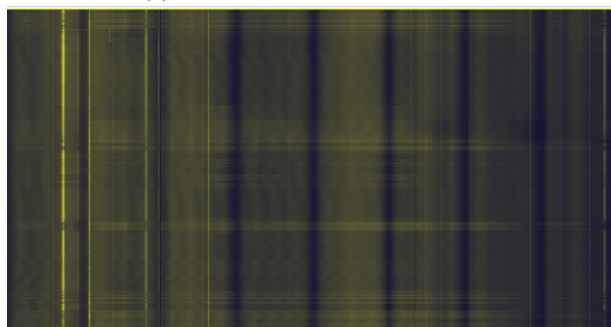
(a) Spectrogram 10th July 2015



(b) Spectrogram 25th June 2015



(c) Spectrogram 24th June 2015



(d) Spectrogram 23rd June 2015

Fig. 33: 24MHz - 40MHz Spectrograms of rtl_power data plotted using heatmap.py

Implementing a HackRF Compatible Flow-Graph in GNURadio

As mentioned previously there is currently no existing tool which is capable of generating spectrogram plots using a HackRF transceiver from previously saved data. In order to rectify this, the methods of generating spectrograms was investigated. One method requires that the digital signal is broken up into chunks of the original bandwidth, and measured using a total power meter. It is not possible to measure the power at an individual frequency, a band of frequencies must be measured instead [Keen, 2015].

Figures. 15 and 45 on pages 22 and 66 shows how a signal is stored digitally once sampled as an I/Q plot. Each data point stored contains the in phase component and the quadrature phase component. The equation shown in Figure. 34 on page 56 can be used in order to calculate the total noise power from such a I/Q digital sample [Nelson, 2015].

$$\text{Power} = I^2 + Q^2 \quad (22)$$

Fig. 34: Converting in-phase and quadrature-phase to power values

The equation listed in Figure. 34 on page 56 has been implemented in within a GNURadio flow-graph and contains a software implementation of a total power radiometer [Nelson, 2015]. The functionality of a radiometer or total power meter provides the means to measure a chunk of bandwidth from a sample and produce a total noise power value which can then be plotted or used elsewhere within a larger GNURadio flow-graph.

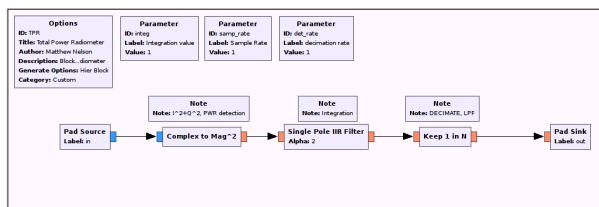


Fig. 35: Total Power Meter Implemented in GNURadio [Nelson, 2015]

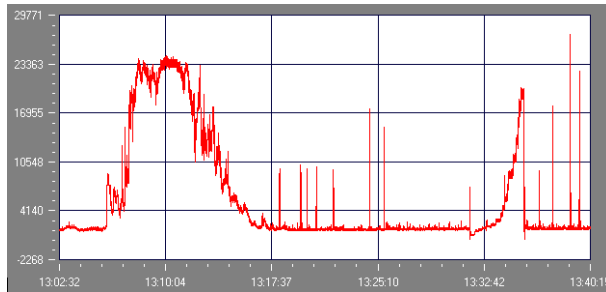


Fig. 36: Radio Skypipe Software Power Plot [Radio-Sky-Publishing, 2015]

Methodology

The following methodology was followed during this experiment:

1. Design a GNURadio flow-graph prototype to generate a set of test signals
2. Design a GNURadio flow-graph prototype to which filters a signal using a bandpass filter
3. Design a GNURadio flow-graph which incorporates the total power meter in order to produce a power plot

The Figure. 36 on page 57 shows a voltage power graph generated using the Radio Skypipe software [Radio-Sky-Publishing, 2015]. Such a graph can be produced by measuring the power from a band of frequency and plotting the values against time. A prototype GNURadio flow-graph (Figure. 38a on page 59) was designed which generates a test signal as seen in Figure. 38b on page 59. This signal was then passed through a bandpass filter, which removes signals outside the permitted frequency range, the result of which can be seen in Figure. 38c on page 59.

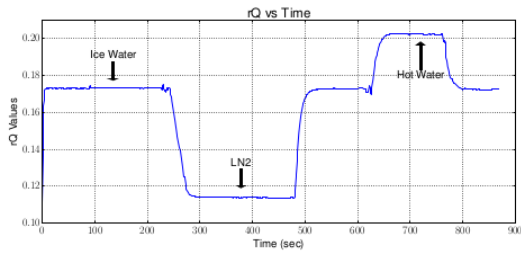
This flow-graph provided the means to isolate and measure the power for individual bands of frequency while ignoring frequencies outside this range. This flow-graph (Figure. 38e on page 59) was then upgraded to incorporate the total power meter as seen in Figure. 38d on page 59. It is possible to capture live power data within a frequency band directly from a osmocom source such as the HackRF, or alternatively from previously recorded data.

A power graph was generated from I/Q data collected during the 20th March 2015 for the solar eclipse radio propagation experiment. The plot shows the signal power (V) rise as the eclipse reaches max totality and can be seen in Figure. 38f

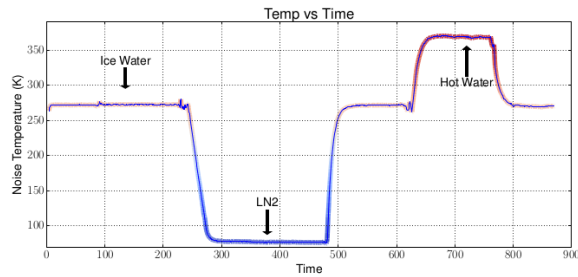
on page 59, which compliments the previously generated signal power (dB) plot shown in Figure. 22a on page 35.

Radiometers can be used to produce signal intensity plots and thereby allow the detection of very faint natural radio emissions such as the Jovian DAM emissions, cosmic microwave background and other discrete astronomical sources such as galaxies [Condon and Ransom, 2010]. In order to make use of a radiometer attached to the telescope for radio astronomical applications it must first be calibrated. Nelson [2015] suggested the use of 3 sources with known temperatures as demonstrated in Figure. 37b on page 58 in order to calibrate the radiometer.

Nelson [2015] collected measurements while the radiometer was immersed in ice water. Next the load was placed in the liquid nitrogen bath and finally in boiling hot water. A linear algebra model was developed in order to convert the total power readings to Kelvin values thereby calibrating the data. Figure. 37b on page 58 shows the calibrated values [Nelson, 2015].



(a) Graph of uncalibrated noise temperature [Nelson, 2015]



(b) Graph of calibrated noise temperature [Nelson, 2015]

Fig. 37: Calibration of the SDR Radiometer

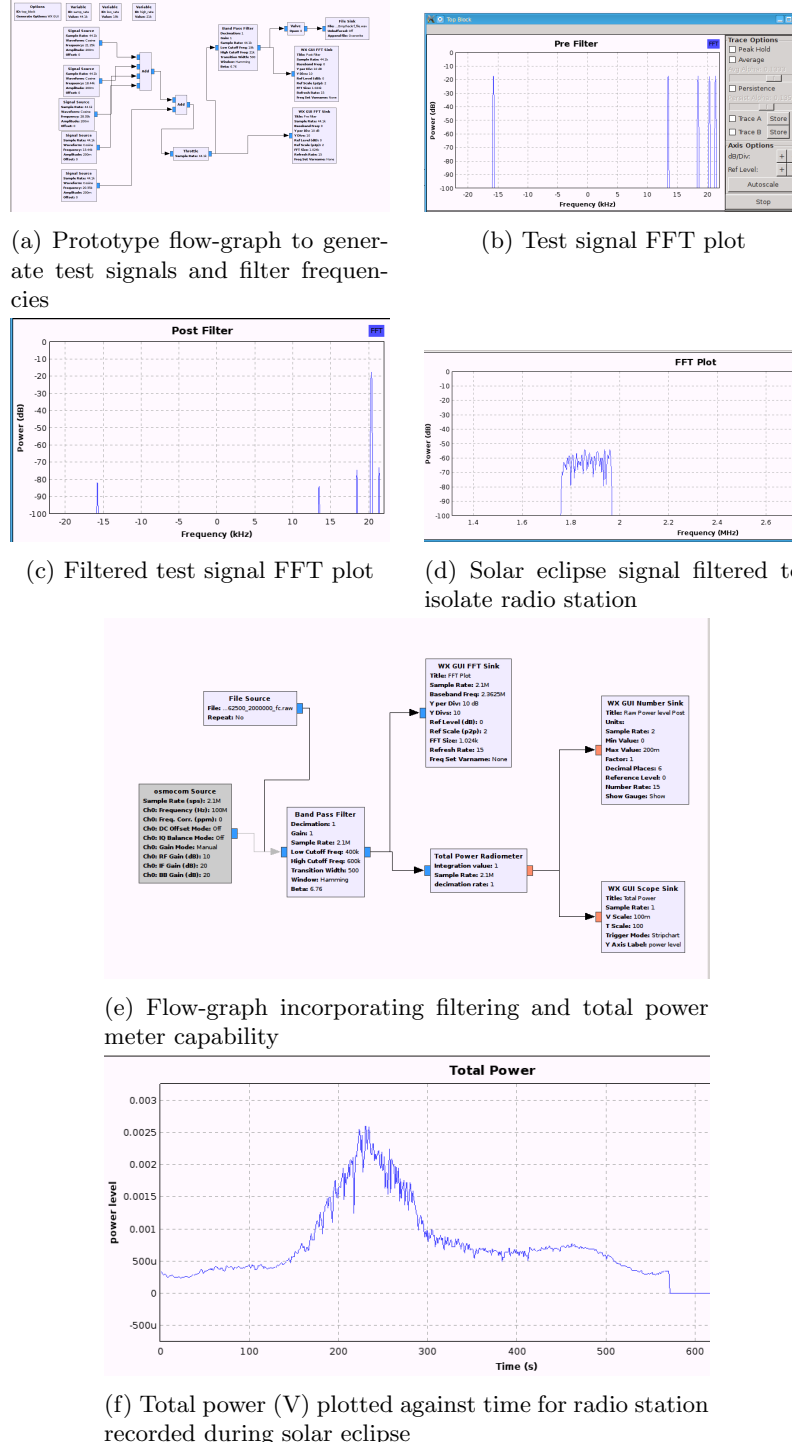


Fig. 38: GNURadio flow-graphs to generate total power plots from saved data

Conclusions

This thesis presented a contribution to the use of software defined radio within amateur radio astronomy. The hypothesis of this thesis is that it is possible to design and construct a low cost radio telescope which is capable of capturing Jovian storm emissions in the DAM frequency range. The chosen antenna design is based on the NASA Radio Jove project while a software defined radio receiver such as the HackRF or RTL DAB system is used in place of the custom hardware offered in the Radio Jove kit. This hypothesis lead to the development of a suite of open source tools and resources which an amateur radio astronomer on a budget might utilise. All software developed is released under the GNU General Public Licence 2.0 and released on Github at: https://github.com/davidkirwan/software_defined_radio_telescope

The research questions presented in Chapter 1 and how they were answered in the thesis are now reviewed.

What current Internet of Things (IoT) technologies would best suit the development of a software defined radio signal listening station and how cheaply can it be created?

This question was partly answered in Chapter 2 the radio antenna build and the special resources required in order to perform a site suitability survey was discussed. An opportunity to be involved in a public radio propagation experiment during the March 2015 solar eclipse aided in the verification of the software defined radio receiver, while the antenna was verified by capturing potential instances of DAM emissions were recorded during an optimal observation period.

Other aspects of this question was answered in Chapter 3. A process for determining the electrical power requirements of an off grid listening site was discussed in Chapter 3. Appropriate capacity sizing to provide adequate power to run the listening site for extended periods using solar renewable solution to charge batteries was also discussed. The computational and networking requirements were also determined for a system capable of performing the necessary functions of a radio telescope listening station.

What processes or algorithms need to be developed to filter or flag known instances of human interference from radio signal observations?

In Chapter 4, the system for flagging occurrences of amateur radio transmissions was developed, it made use of the global DXCluster systems which

the amateur radio enthusiast community use to share information regarding transmissions which were observed. A system for flagging occurrences of natural interference from lightning strikes was also developed. The system makes use of data gathered from the Blitzortung global lightning detection system to identify lightning strikes which occur within a certain range of the listening site.

What SDR tools, processes and or algorithms need to be developed to identify instances of the three main DAM emission types detailed in Table. 1?

Chapter 5 demonstrated the process of generating spectrograms from data recorded using the RTL DAB receiver. Spectrograms provide the means to visualise large portions of the radio spectrum over long periods, in the hope of identifying periods of Jovian storm activity in the DAM range. A GNURadio flow-graph was developed in order to generate power plots using a radiometer implemented in SDR. Radiometers are used to measure the signal intensity of radio emissions and are a standard tool in the radio astronomer toolbox. A radiometer could be used to find evidence of the DAM emissions in data which they might otherwise be invisible.

Future Work

The future work section is broken up into the following research areas:

Filtering Human Signal Interference

It is envisioned the time and frequency values associated with this data related to amateur radio enthusiast signals, could be overlaid on top of the spectrogram diagram generated by heatmap.py. This could be performed on the previous 24 hours worth of data collected by the telescope, or potentially in real time as information is collected and processed.

Filtering Natural Interference

An overlay similar to that for the natural signals could be generated using data collected from the Blitzortung server, which may aid in the identification of wide spectrum interference related to lightning strikes. The existing Blitzortung client is an initial skeleton implementation and requires further development. The current design needs human intervention at several points in order to ensure the processing of data. The development of a full client for interacting with

the Blitzortung server would also need approval from the Blitzortung system administrators, as it could potentially add damaging load to the system. It was for this reason the client was not fully automated, manual control ensured excessive load was not put on the server.

Creating Spectrograms with HackRF

It was infeasible to reproduce a system as complex as rtl_power in order to make it compatible with the HackRF transceiver within the scope of this dissertation. It was possible however, to initiate this process by replicating a number of discrete functions which rtl_power performs in order to produce spectrograms. In Chapter 5 the ability to filter a band of the radio spectrum in GNURadio to exclude unwanted frequencies using SDR band pass filters to take power measurements was implemented. The rtl_power utility automates this functionality across a spectrum.

The GNURadio flow-graph could be further developed to replicate the functionality of rtl_power by automating the filtering of each subsection, measure the power the SDR radiometer before shifting focus to the next section of the frequency band. Power data could then be outputted in a format which would be compatible with the heatmap.py utility for generating spectrograms.

Calibrating the SDRT for Accurate Power Measurements

Until such time as the SDRT is calibrated, the signal intensity measurements are meaningless as they are not in a quantitative data form. The formula shown in Figure. 40 on page 63 provides the means to calibrate the radio telescope. The cosmic microwave background value T_{cmb} approximates to 2.73 K, T_{source} is the radio source, T_{atm} is the added interference from the atmosphere $T_{spillover}$ relates to the emissions entering the receiver from outside the antenna beam while the T_{rcvr} accounts for the noise generated within the receiver itself.

$$k \approx 1.38 \times 10^{-23} \text{ JouleK}^{-1} \quad (23)$$

$$T_N \equiv \frac{P_v}{k} \quad (24)$$

Fig. 39: Converting Power(V) to Temperature(K)

In the formula contained in Figure. 39 on page 62, k is the Boltzmann constant and T_N is the noise temperature while P_v is the power value measured by the radiometer. Using this formula it is possible to calculate the noise temperature value (K) for a noise source power value (V) [Condon and Ransom, 2010]. Once calibration is complete it would then be possible to take accurate readings using the SDRT system [Condon and Ransom, 2010]. Alternatively the telescope could be calibrated using the Radio Skypipe software with the help of a hardware calibration tool offered by the Radio Jove organisation [Radio-Sky-Publishing, 2015] [NASA, 2010].

$$T_{sys} = T_{cmb} + \Delta T_{source} + T_{atm} + T_{spillover} + T_{rcvr} \quad (25)$$

Fig. 40: Calibration of Telescope Total Noise Power

Automated Detection of DAM Emissions

It is feasible a machine learning neural network could be developed which could be used to automatically identify DAM emissions from signal intensity plots, or perhaps from spectrograms. Interference emission data collected by the utilities developed in Chapter 4 might feed into and help train such a neural network.

Final Summary

In conclusion while this research was necessarily limited by the available time and resources, never the less a contribution to new knowledge was made through the development of supporting open source tools and resources which might enable further research in this field in the future. There are several existing large radio telescope arrays, such as the Atacama Large Millimeter/submillimeter Array (ALMA), while several others are already under construction such as the Low Frequency Array (LOFAR) or in the early planning stages and are due to be built in the near future like the Square Kilometre Array (SKA). I am encouraged to continue working on this and similar topics, and the possibility of applying to a doctoral program which might allow the pursuit of a research career in astronomy is currently being considered.

Appendix

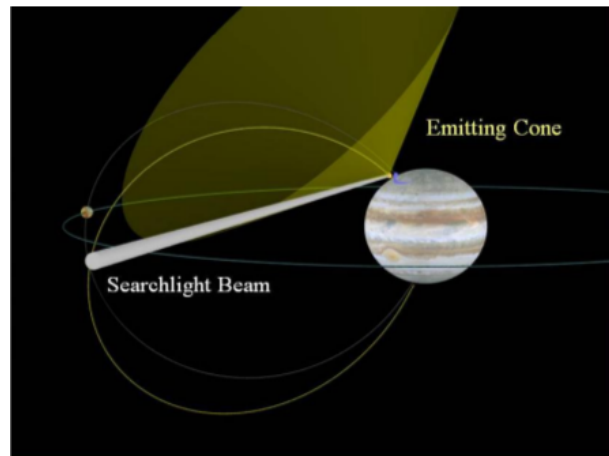


Fig. 41: A searchlight beam model of Jupiter's decametric radio emissions [Imai et al., 2008]

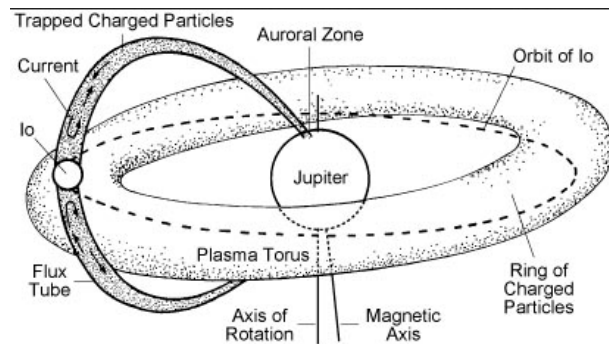
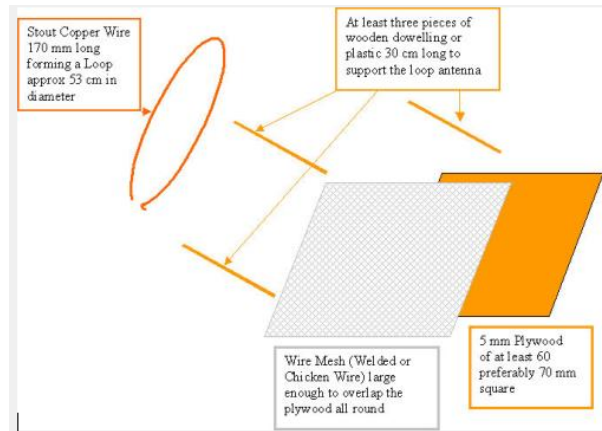


Fig. 42: Io Flux Tube and the Plasma Torus [Lang, 2010]



(a) 21 MHz Shortwave Loop Antenna Radio Telescope Design [Greef, 2012]



(b) 21 MHz Shortwave Loop Antenna Radio Telescope Design [Greef, 2012]

(c) 21 MHz Shortwave Loop Antenna Radio Telescope Design [Greef, 2012]

Fig. 43: 21MHz Shortwave Loop Design

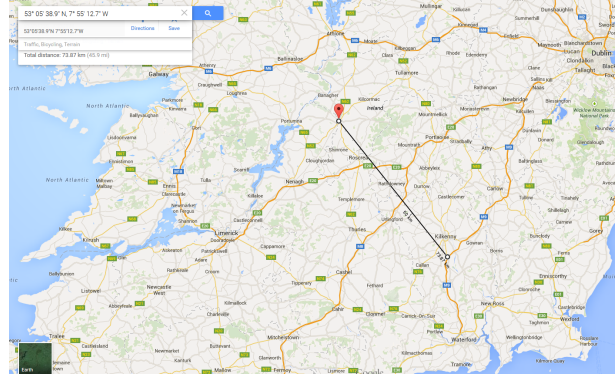
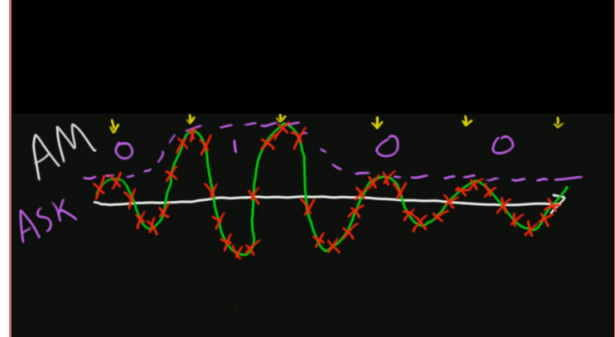
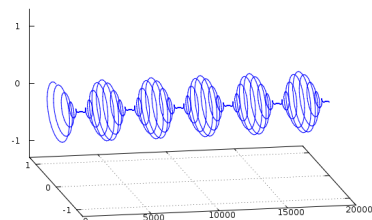


Fig. 44: Distance between the Birr and Kilkenny site survey

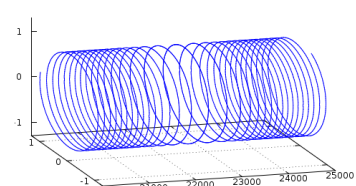
(a) Sampling an Analogue Amplitude Modulation Signal
[Ossmann, 2015c]

AM-modulation in IQ



(b) I/Q Sample Polar Plot of an AM Modulated Signal [Kuisma, 2014]

FM-modulation in IQ



(c) I/Q Sample Polar Plot of an FM Modulated Signal [Kuisma, 2014]

Fig. 45: Signal Modulation

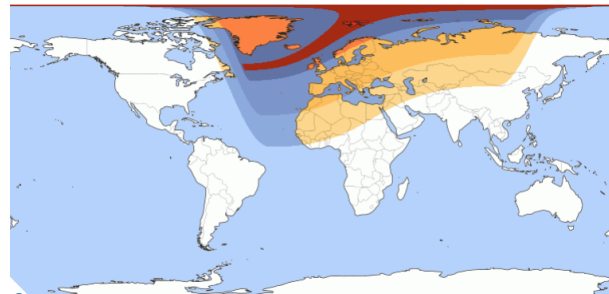


Fig. 46: Partial Solar Eclipse 20th March 2015 [timeanddate.com, 2015]

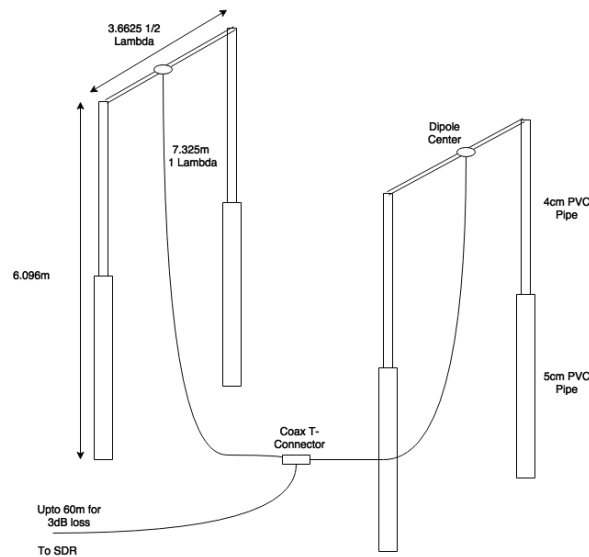


Fig. 47: SDRT Dual Dipole Antenna Design based on NASA RadioJove

Bibliography

- ARRL. *ARRL Operating Manual 7th Edition*, 2000. URL <http://www.arrl.org/shop/ARRL-Operating-Manual-10th-Edition/>.
- Thomas Ashcraft. Jupiter 27 september 2013 n event, September 2013. URL http://www.heliotown.com/Jupiter_Sep272013_N_Event.html.
- John W. Belcher. The jupiter-io connection: An alfvén engine in space. *Science*, 238(Oct 9):170–176, 1987.
- S. K. Bose, S. Sarkar, and A. B. Bhattacharyya. Jovian decametric radio emission: An overview of the planetary radio astronomical observations. *Indian Journal of Radio and Space Physics*, 37:77–108, 2008.
- Michael Bryce. *Emergency Power for Radio Communications*, chapter 3, page 12. ARRL - The national association for amateur radio, 2011. ISBN 978-0-87259-615-3. URL <http://www.arrl.org>.
- F.B. Burke and L. K. Franklin. Obervations of variable radio source associated with the planet jupiter. *Journal of Geophysical Research*, 60(213), 1955.
- Comreg. *Overview Comreg - Radio Spectrum*. Commission for Communications Regulation, 2014. URL http://www.comreg.ie/radio_spectrum/overview.496.html.
- J.J. Condon and S.M. Ransom. Essential radio astronomy - radiometers, 2010. URL <http://www.cv.nrao.edu/course/astr534/Radiometers.html>.
- ECA&D. European climate assessment and dataset, 2015. URL <http://eca.knmi.nl/dailydata/customquery.php>.
- J. M. Freidt. Gnuradio as a digital signal processing environment: Application to acoustic wireless sensor measurement and time and frequency analysis of periodic signals. *Joint UFFC EFTF and PFM Symposium*, pages 278–281, 2013.
- Gnuradio. Tutorials - gnuradio, 2014. URL <http://gnuradio.org/redmine/projects/gnuradio/wiki/Tutorials>.
- B. Greef. A simple decametric radio telescope for jupiter, 2012. URL http://www.ukaranet.org.uk/uk_amateurs/bobgreef/.
- Hamradio-Science. Rtl2832u / r820t vs rtl2832u / e4000, 2012. URL <http://www.hamradioscience.com/rtl2832u-r820t-vs-rtl2832u-e4000/>.
- K. Imai, L. Garcia, F. Reyes, M. Imai, J. R. Thieman, and M. Ikuta. A Search-light Beam Model of Jupiter’s Decametric Radio Emissions. *AGU Fall Meeting Abstracts*, page B1673, December 2008.

- Kyle Keen. Great-circle distance calculations in r, 2015. URL <https://github.com/keenerd/rtl-sdr-misc>.
- M. G. Kivelson, K. K. Khurana, R. J. Walker, C. T. Russell, J. A. Linker, D. J. Southwood, and C. Polanskey. A magnetic signature at io: Initial report from the galileo magnetometer. *Science*, 273, July 1996.
- Dirk Koopman. Dxspider, 2007. URL <http://www.dxcluster.org/main/>.
- Mikael Q Kuisma. *I/Q Data for Dummies*, 2014. URL <http://whiteboard.ping.se/SDR/IQ>. Complex Numbers in DSP.
- K. R. Lang. Io flux tube and plasma torus, 2010. URL http://ase.tufts.edu/cosmos/view_picture.asp?id=1174.
- J Litva and B.J. Rook. *Beverage Antennas for HF Communications, Direction Finding and Over-the-horizon Radars*, chapter 1, pages 1–3. Communications Research Centre, 1976. URL <http://www.nrccdxas.org/articles/BevAnt0876.pdf>.
- Joe McCauley. Craf the esf expert committee on radio astronomy frequencies, 2013. URL http://www.craf.eu/newsletters/newsletter27_0713.pdf.
- MET. Download historical climate data for our synoptic stations, 2015. URL <http://www.met.ie/climate-request/>.
- NASA. *Measuring Antenna Temperature*, 2010. URL <http://radiojove.gsfc.nasa.gov/observing/Measuring%20Antenna%20Temperature%20Jove%20.pdf>.
- NASA. *The Effects of Earth's Upper Atmosphere on Radio Signals*, 2012a. URL <http://radiojove.gsfc.nasa.gov/education/educ/radio/tran-rec/exerc/iono.htm>.
- NASA. *Antenna Kit and Manual Developed for NASA Radio JOVE Project by The Radio JOVE Project Team*, 2012b. URL http://radiojove.gsfc.nasa.gov/telescope/ant_manual.pdf.
- NASA. *Radio Jove Radio Telescope Kit Order Form*, 2014. URL http://radiojove.gsfc.nasa.gov/office/order_form.html.
- Matthew-Erik Nelson. Implementation of a total power radiometer in software defined radios, 2015. URL <https://github.com/matgyver/Radiometer-SDR-Thesis>.
- Steve Nichols. Partial solar eclipse propagation experiment, march 20th 2015, 2015a. URL <http://forums.thersgb.org/index.php?threads/partial-solar-eclipse-propagation-experiment-march-20th-2015.125/>.

- Steve Nichols. Partial solar eclipse propagation experiment, march 20th 2015, 2015b. URL <http://www.g0kya.blogspot.ie/2015/02/partial-solar-eclipse-propagation.html>.
- Michael Ossmann. *Software Defined Radio with HackRF*, 2015a. URL <http://greatscottgadgets.com/sdr/>.
- Michael Ossmann. *Software Defined Radio with HackRF*, 2015b. URL <http://greatscottgadgets.com/sdr/9>. Aliasing.
- Michael Ossmann. *Software Defined Radio with HackRF*, 2015c. URL <http://greatscottgadgets.com/sdr/7>. Complex Numbers in DSP.
- Michael Ossmann. *Software Defined Radio with HackRF*, 2015d. URL <http://greatscottgadgets.com/hackrf/>. HackRF One.
- Mario Pineda-Krach. Great-circle distance calculations in r, 2010. URL <http://www.r-bloggers.com/great-circle-distance-calculations-in-r/>.
- Radio-Sky-Publishing. *Radio Jupiter Pro*, 2014. URL <http://www.radiosky.com/rjpro3ishere.html>.
- Radio-Sky-Publishing. *Radio Skypipe Pro*, 2015. URL <http://www.radiosky.com/skypipeishere.html>.
- RSGB. *RSGB Radio Communication Handbook*, 2014. URL http://www.rsgbshop.org/acatalog/Online_Catalogue_Technical_6.html.
- Steven W. Smith. *Digital Signal Processing A Practical Guide for Engineers and Scientists*, chapter 1, pages 1–3. Newnes, 2003a. ISBN 0-75067444-X. What is DSP.
- Steven W. Smith. *Digital Signal Processing A Practical Guide for Engineers and Scientists*, chapter 3, pages 39–44. Newnes, 2003b. ISBN 0-75067444-X. Sampling Theorem.
- Superkuh. Radio spectrum, 2007. URL http://superkuh.com/radio/2014-08-26_17-55_70-1000_25k/.
- timeanddate.com. Total solar eclipse - kilkenny, ireland, 2015. URL <http://www.timeanddate.com/eclipse/in/ireland/kilkenny?iso=20150320>.
- E. Wanke, R. Andersen, and T. Volgnandt. *A WorldWide Low Cost Community Based Time of Arrival Lightning Detection and Lightning Location Network*, 2014. URL http://www.blitzortung.org/Documents/TOA_Blitzortung_RED.pdf.
- M. Wilkinson and J. Kennewell. A project to detect radio emissions from jupiter. *Southern Sky*, 1994. URL <http://www.spaceacademy.net.au/spacelab/projects/jovrad/jovrad.htm4>.